Nasa CR-65234

SECOND QUARTERLY REPORT

Thin-Film Personal Communications and Telemetry System (TFPCTS)

Contract No. NAS 9-3924

Submitted to

NATIONAL AERONAUTICS AND SPACE ADMINISTRATION
MANNED SPACECRAFT CENTER
Houston, Texas

MELPAR, INC.
7700 Arlington Boulevard
Falls Church, Virginia

Second Quarterly Report

THIN-FILM PERSONAL COMMUNICATIONS AND TELEMETRY SYSTEM (TFPCTS)

For the period of March 21, 1965 to June 21, 1965

Contract No. NAS 9-3924

July 1965

Submitted to

National Aeronautics and Space Administration
Manned Spacecraft Center
Houston, Texas

Submitted by

Melpar, Inc.
7700 Arlington Boulevard
Falls Church, Virginia

TABLE OF CONTENTS

LIST OF ILLUSTRATIONS

LIST OF ILLUSTRATIONS (Continued)

LIST OF TABLES

1. INTRODUCTION

This Second Quarterly Report is submitted in compliance with Contract NAS 9-3924. Phase A of this contract is a research effort to develop thin-film active devices and passive circuit elements for use at ultrahigh frequencies. The thin-film components will be used in the design of a Thin-Film Personal Communications and Telemetry System (TFPCTS) in monotronic form.

At this time, there have been no unexpected problems or delays. Work is progressing smoothly in accordance with the PERT time table, which is presented in an up-to-date version at this six-month point in phase A. The revised PERT Chart has the appropriate bubbles shaded to indicate approximately the various states of completion of each task.

The areas of effort are outlined in this report in the same manner as the First Quarterly Report. The exception is the "High-frequency Substrate Investigation." which was completed in the First Quarterly Report. The "Dielectric Investigation" is completed in this report. Substrates and capacitors have been determined to be very satisfactory in performance at frequencies above 300 megacycles per second.

The work on new semiconductor materials for high-frequency field-effect triodes has lead to field effect being observed in many new or untried materials. The next step in the development of a high-frequency thin-film triode in phase A is the selection of the most promising thin-film semiconductors and their intensive and exclusive investigation. This event is shown on the PERT Chart in the TFT Formation line in the Selection

of Semiconductor Materials bubble. The most promising of the "new" materials seems to be CdTe. The thin-film semiconductors which have been used to form the most successful TFTs are CdSe, CdS, and Te. Although these last-mentioned semiconductors have been extensively used, their thin-film electrical parameters have by no means been optimized. It is the opinion of researchers in this laboratory that these materials, CdTe, CdSe, CdS, and Te, in conjunction with a suitable device geometry, hold the most promise of fabricating a high-frequency thin-film triode. Therefore, the work in this area will now be concentrated on the vacuum-deposition techniques for optimizing the thin-film electrical parameters of these four semiconductor materials.

The metal base transistor research effort has been predominantly the optimization of the formation of junctions. These junctions have been successful in that their parameters are comparable in most aspects with commercial p-n junction diodes. Therefore, the effort on diodes which was scheduled to begin in the 30th week of this contract was incorporated with the metal base transistor effort and begun this quarter.

The inductor effort, which has long passed its scheduled work effort, seems to lead continually to further investigations. Work in this area, therefore, will continue. Ferrite films are promising in that a type of ferrite is actually being formed through the use of vacuum-deposition techniques exclusively. More research and classification are necessary before any final conclusions can be drawn. This effort, as indicated on the PERT Chart, has been extended from 36 weeks (40 man-weeks) to 40 weeks (45 man-weeks) to ensure a thorough investigation.

Detailed accounts of progress during this quarter are presented in the following sections.

CuTouT 1

E2734

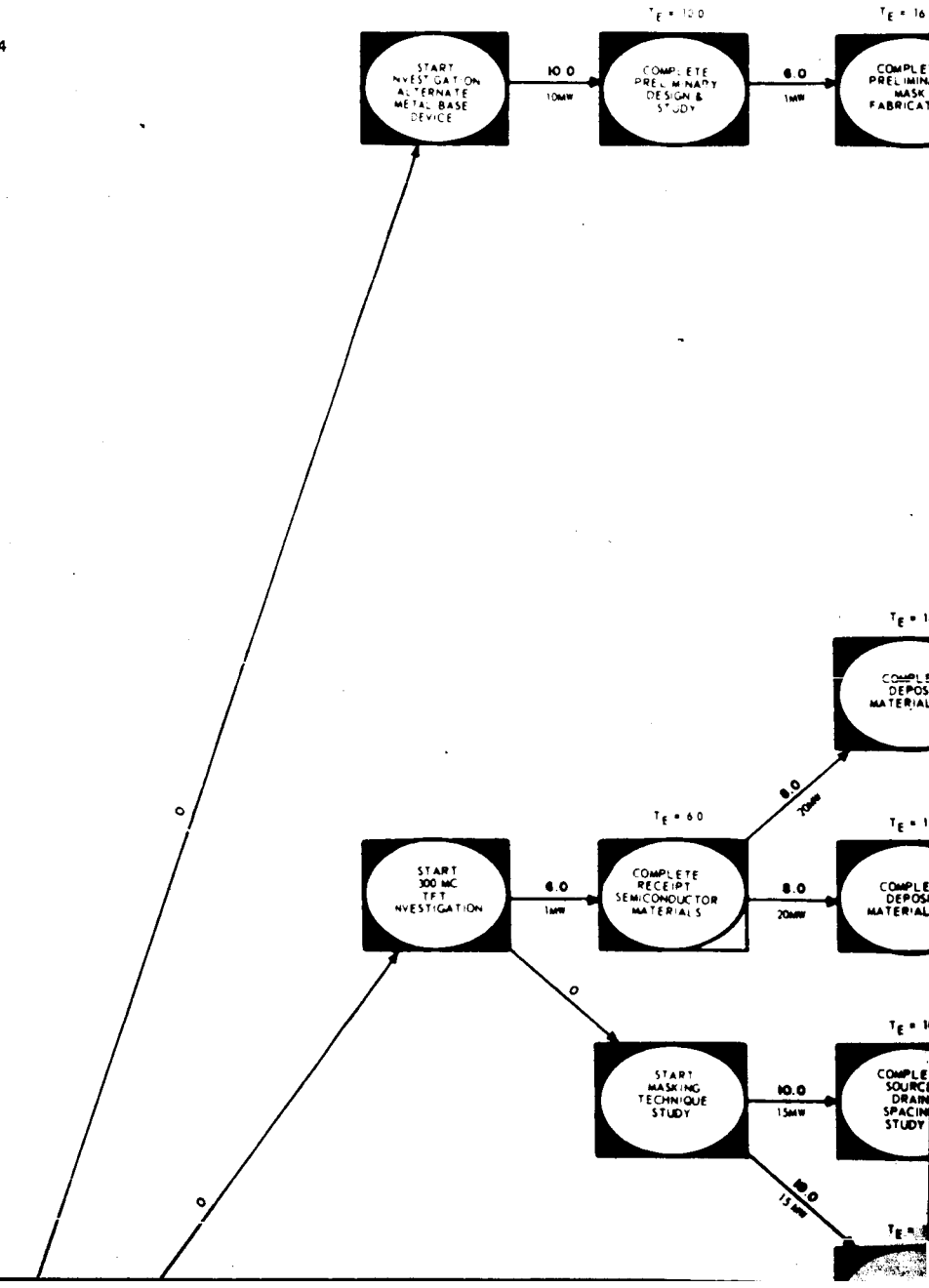

Page 8
Cutout 2

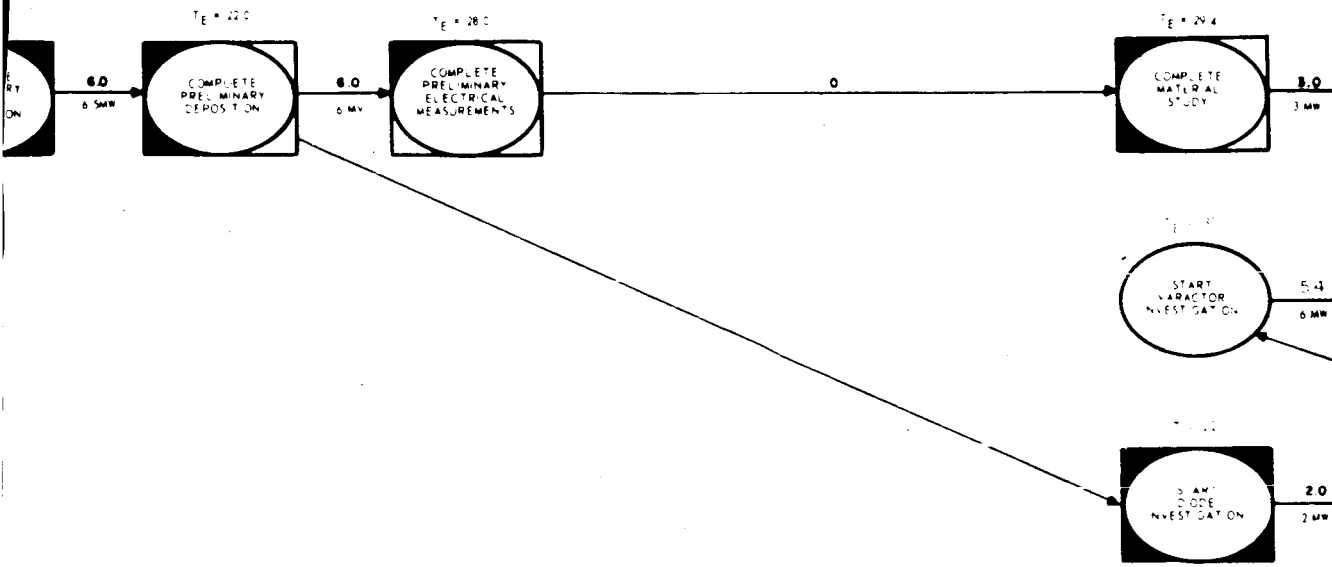

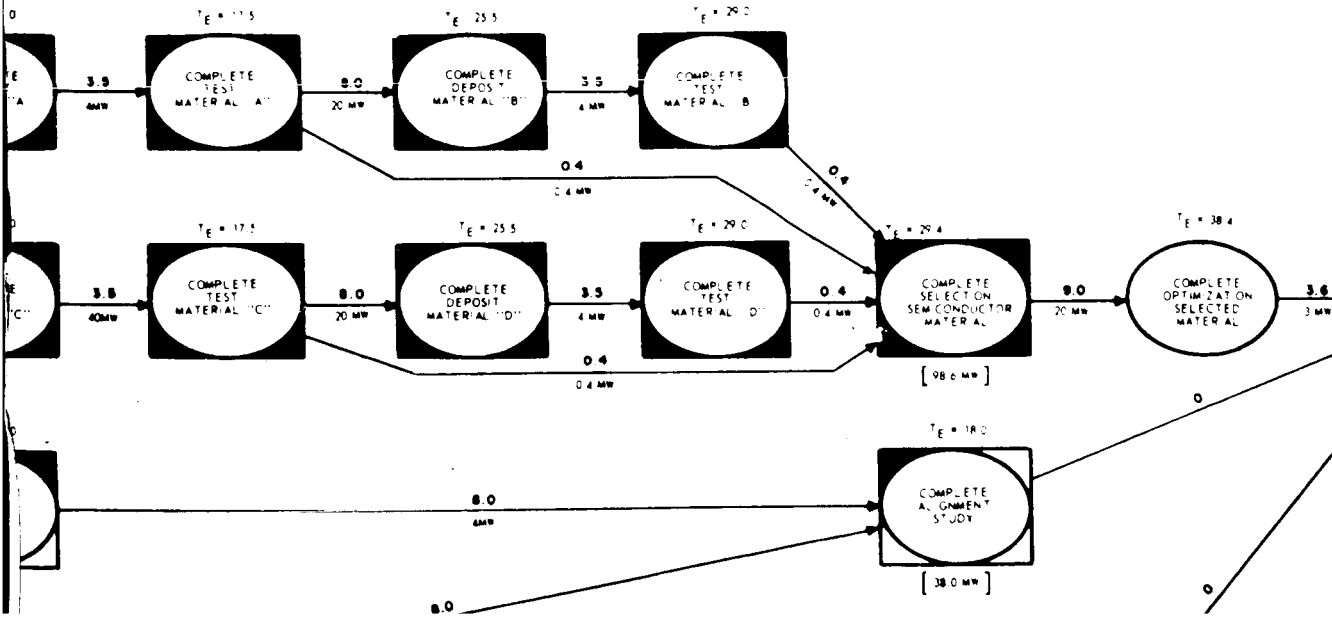

PAGE 8
CUTOUT 3

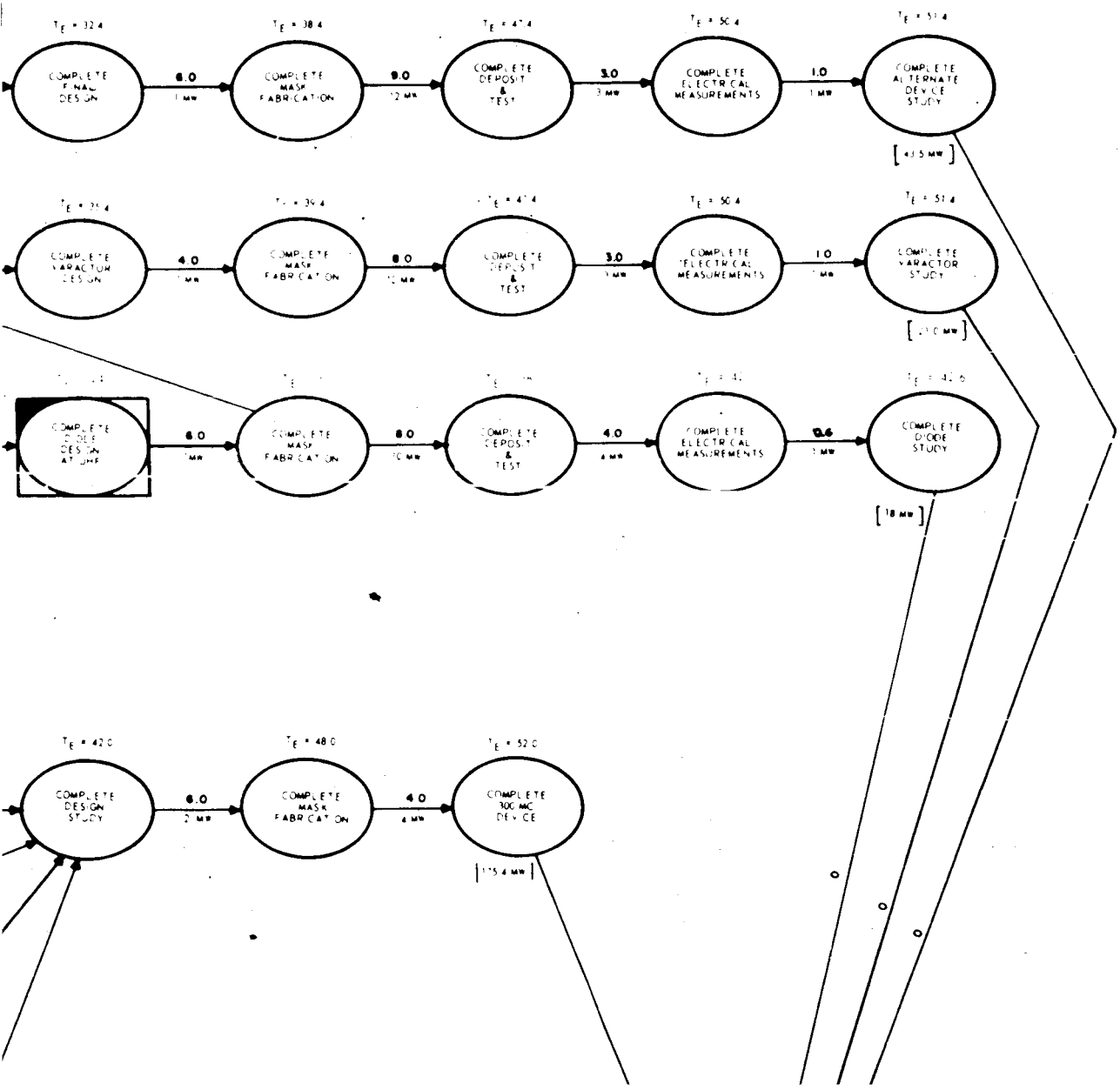

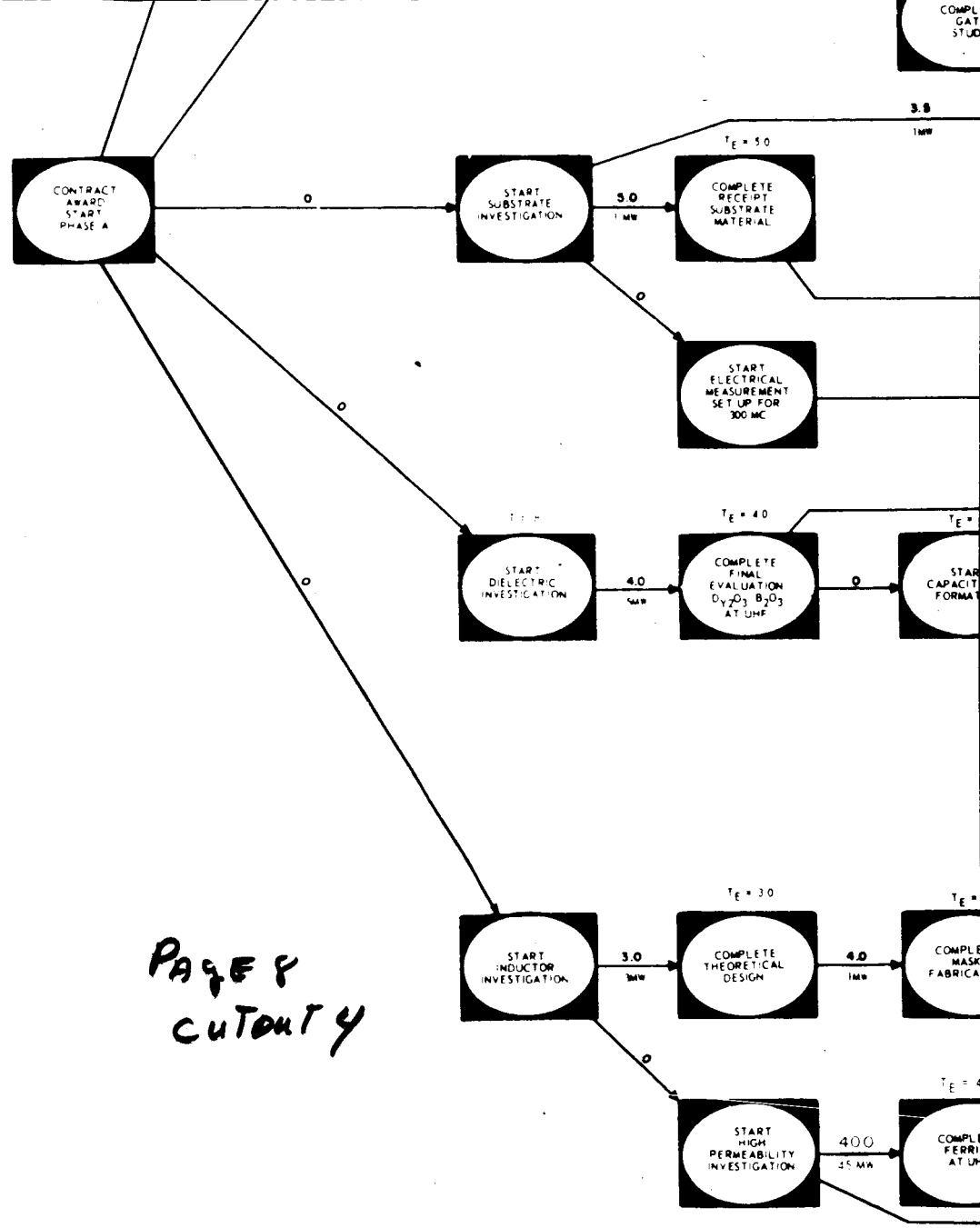

PAGE 8
CUTOUT 4

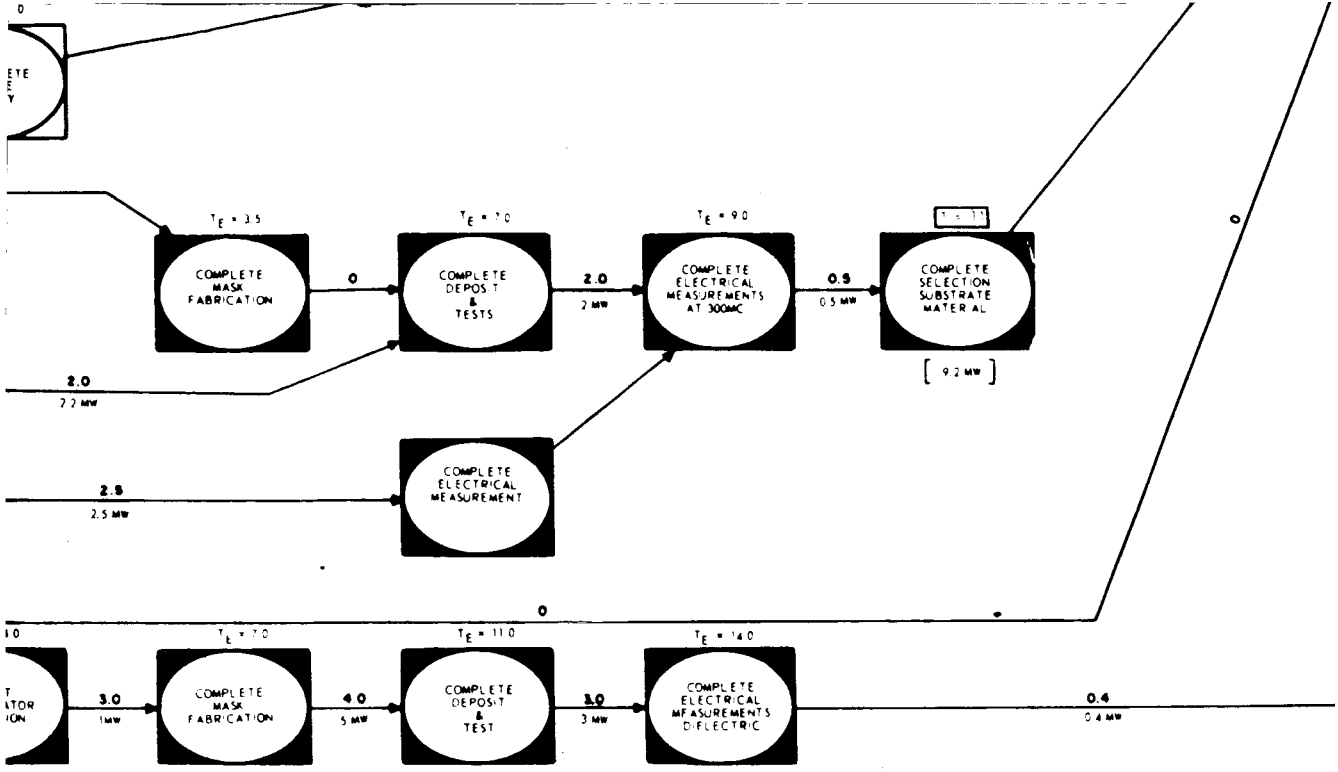

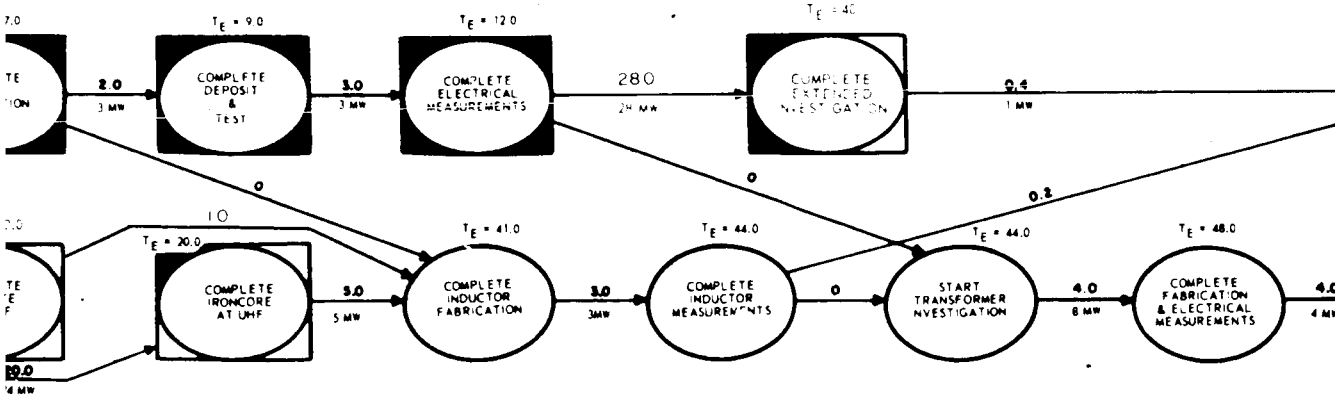

PAGE 8
CUTOUT 5

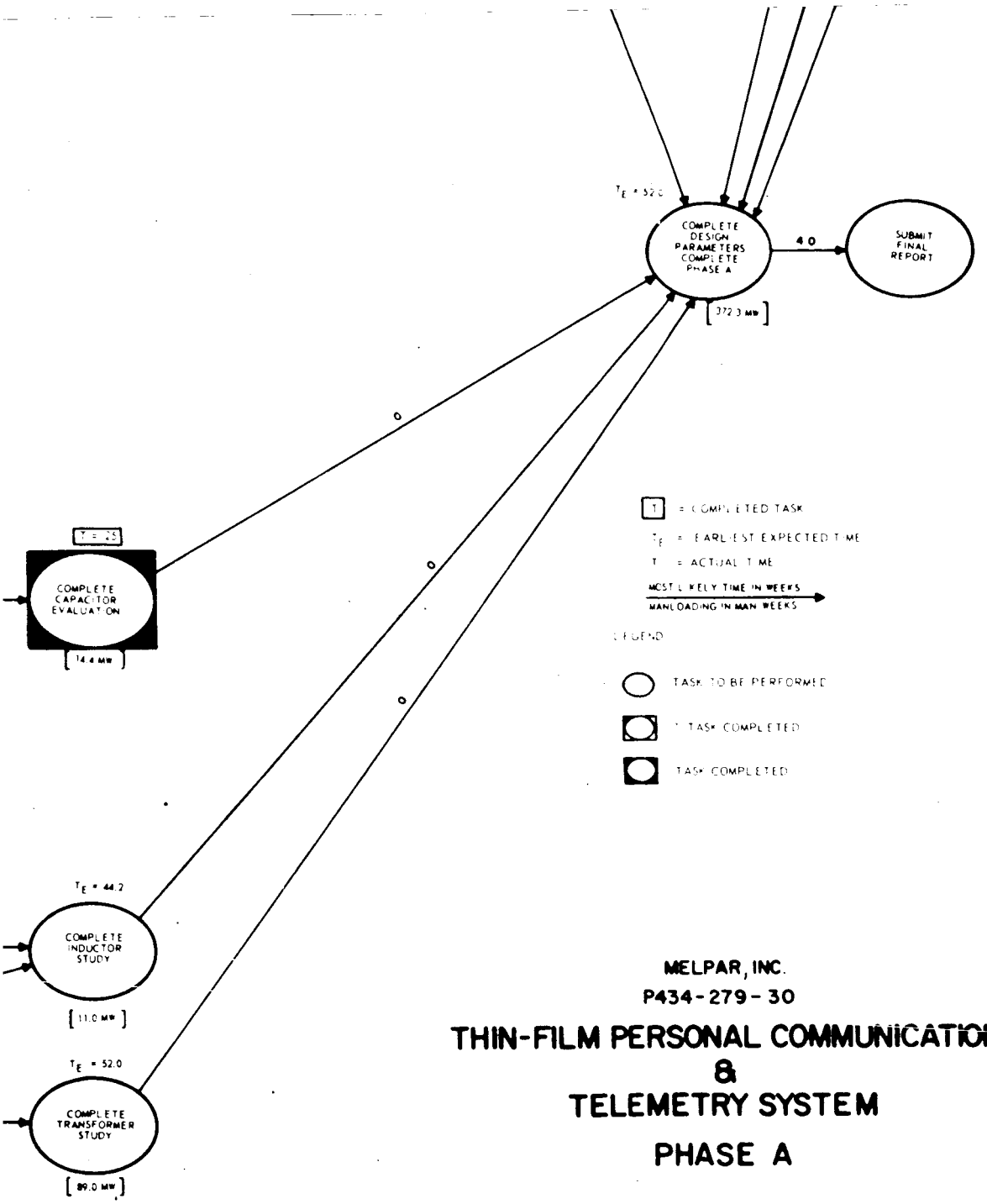

MELPAR, INC.

P434-279-30

THIN-FILM PERSONAL COMMUNICATION & TELEMETRY SYSTEM PHASE A

CUTOUT 6

2. HIGH-FREQUENCY THIN-FILM TRIODES

During this quarter, several different semiconductor materials were initially investigated. The electrical measurements considered are Hall effect and field effect (drift mobility). These measurements are the most useful for evaluating semiconductor films for use in thin-film field-effect triodes (TFTs). The materials studied were cadmium telluride (CdTe), silver telluride (Ag_2Te), bismuth telluride (Bi_2Te_3), lead telluride (PbTe), manganese telluride (MnTe), tin sulfide (SnS), bismuth selenide (Bi_2Se_3), and manganese selenide (MnSe). These materials were obtained from Penn Rare Metals, Kern Chemical Co., and K & K Laboratories.

The basic vacuum-system setup reported for Te evaporations in Quarterly Report No. 1 (Fig. 3, p. 15) was used for depositing the semiconductor films discussed here.

Corning glass substrates (code 0211, 10 mils thick) were used. Nichrome source-drain electrodes were deposited 1500 Å thick with a source-drain spacing 0.5 mil and 100 mils in length (1/200 square).

The semiconductor films were deposited from a molybdenum boat using 50-mg charges of material. The usual procedure was to precede the deposition by a substrate outgassing in vacuum (10^{-6} mm Hg) at 400°C for five minutes, followed by a 30-minute cooling period. At the time of semiconductor deposition, the substrates were at a temperature of 40°C.

An SiO deposit of 1500 Å thick, followed by a 500 Å Al gate electrode, was used to complete the device structure to observe device characteristics utilizing the semiconductor layers listed.

Work is also being continued with the semiconductors which are known to form successful TFTs: tellurium (Te), cadmium sulfide (CdS), and cadmium selenide (CdSe). The optimization of these films presents the most promising approach to the fabrication of high-frequency TFTs.

2.1 Properties of Semiconductor Films Initially Investigated

Cadmium Telluride

The evaluation of these films indicated that the rate of deposition determined by the source-boat temperature greatly affected the film electrical properties. Films deposited from a boat held above 600°C, which resulted in a film-growth rate greater than 300 Å per second, were found to be very high in resistivity. Films deposited from a boat heated in the range of 300° to 500°C resulted in rather low resistivity. It is suspected that, in the latter case, the films are primarily disassociated Te. This is based on the expected resistivity range found in pure Te deposits, and that the unevaporated charge residue was found to be a yellowish color, signifying excessive cadmium content. The films exhibited "p"-type conductivity.

At higher boat temperatures, it is believed that the films are deposited with a closer stoichiometric ratio of 1 to 1 for the two elements forming the compound. To form an "n"-type deposit from a CdTe charge, an excess of cadmium or other material may be necessary.

Figure 1 illustrates the electrical characteristics of a CdTe TFT as observed on the 575 (Tektronix) curve tracer. Operation with both plus and minus drain voltage and positive and negative gate stepping is demonstrated through the use of a double-exposure photograph.

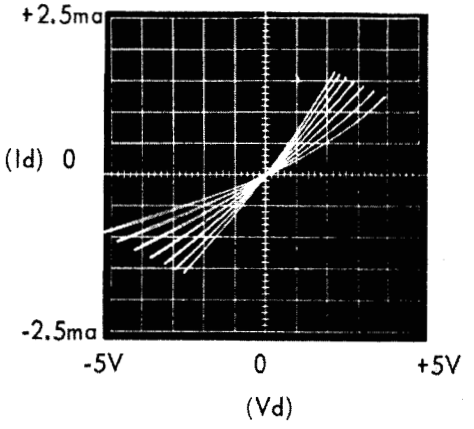

Figure 1. Characteristics of CdTe TFT

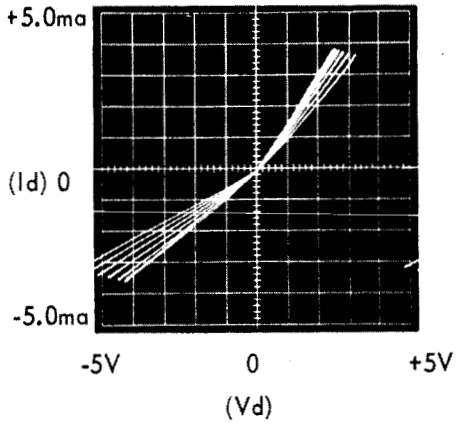

Figure 2. Characteristics of PbTe TFT

This device was formed by depositing CdTe from a boat held at 400°C during the evaporation. As may be seen, "pinchoff" is not achieved in either the positive or negative direction. In general, the characteristics observed were similar to poor-quality Te devices.

Lead Telluride

Film resistivity was found to be considerably less dependent on the rate of deposition than for CdTe layers. A boat temperature of 500°C was used to deposit films of 200Å at a rate of 50Å per second. Figure 2 illustrates electrical characteristics observed on the curve tracer. Again, the general characteristics observed were similar to poor-quality Te devices.

Silver Telluride

Films were deposited from a boat held at 500°C during the evaporation at a rate of approximately 50Å per second. Films deposited to a thickness of 2000Å exhibited Hall mobilities of up to 400 cm^2/volt sec. Higher mobility could be obtained with thicker films. Unfortunately, the relatively high mobility figure could not be taken advantage of because films of such thickness exhibited very little, if any, field effect, which is probably due to the large number of carriers. Electrical parameters and the Hall measurements indicate that the films are "n" type (particularly for the thicker films), thereby giving indication that they may have compound properties and are not predominated by elemental tellurium, which is normally "p" type in film form.

Characteristics of completed TFTs utilizing thin Ag_2Te_3 films of approximately 500Å could be observed as shown in figure 3. Almost compatible operation in the negative and positive areas indicates that the semiconductor layer is neither strongly "p" nor "n" type in conductivity.

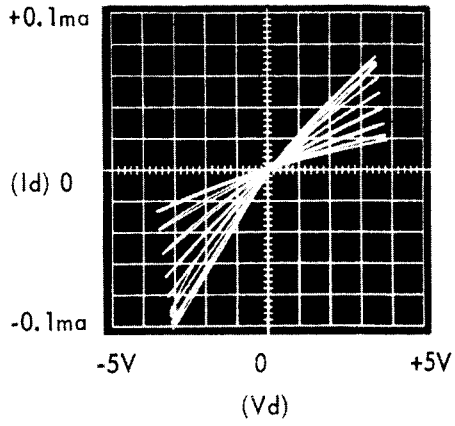

Figure 3. Characteristics of Ag_2Te_3 TFT

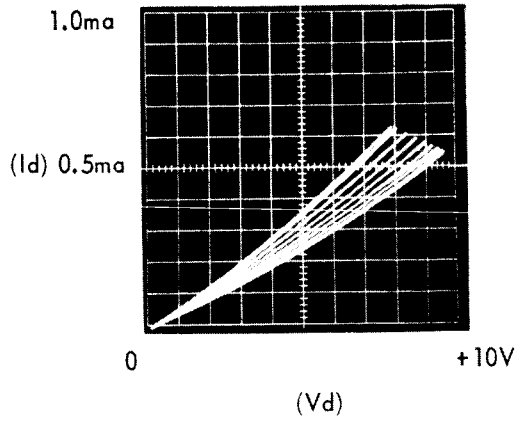

Figure 4. Characteristics of Bi_2Se_3 TFT

Bismuth Selenide

Films deposited from a bismuth selenide charge were generally very low in resistance, regardless of evaporation rate. A boat temperature of 600°C for a period of 1 minute resulted in a film 200Å thick. This film was given a slight anneal at 150°C for five minutes before withdrawing from vacuum. (The tellurides listed here will re-evaporate or diffuse entirely if heated in vacuum to temperatures greater than 100°C for periods of five minutes or more.) Characteristics of the complete device, utilizing the film described, are shown in figure 4. Care was taken to ensure that the curves illustrated were not merely dielectric breakdown which may illustrate a similar pattern. In general, field effect was very poor and no Hall mobility could be detected. The conductivity type is usually "n."

Bismuth Telluride

Bismuth telluride films exhibited very low resistivity regardless of rate of deposition (boat temperature). No field effect was detected in these first films formed. Neither Hall mobility nor conductivity type could be detected.

Manganese Selenide

A boat temperature of 1000°C was required to obtain a deposition rate of 50Å/sec. Film thicknesses of approximately 1700Å were studied in device structures. Hall mobility was not detectable. Figure 5 illustrates the electrical field-effect characteristics observed in a completed device.

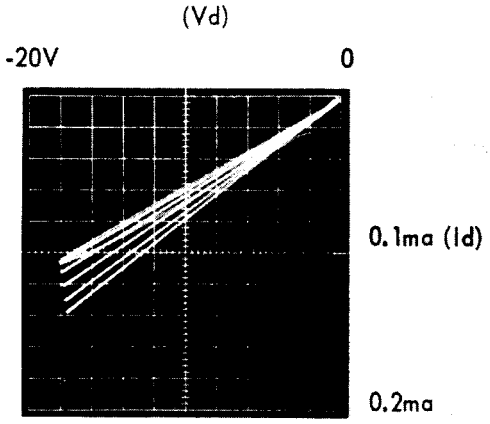

Figure 5. Characteristics of MnSe TFT

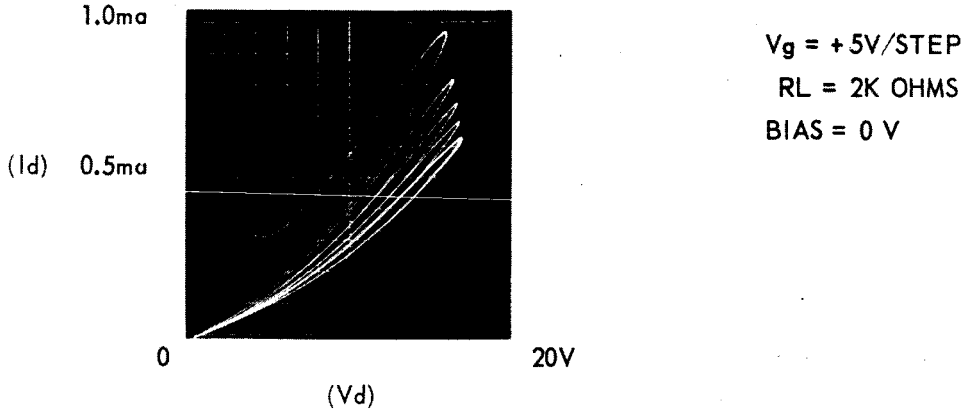

Figure 6. Characteristics of MnTe TFT

Manganese Telluride

A boat temperature of 400°C was sufficient to deposit films from this material at a rate of 100Å per second. Films studied were approximately 1000Å thick. See figure 6.

Hall mobility was very low for these films unless a post bake in air at 300°C for two minutes was performed. In films treated with the post bake, Hall mobilities of up to 40 cm^2/volt sec were measured. The post bake and the resulting higher mobility obtained, however, did not improve the field effect noted. The post-bake films indicated "p" type conductivity in Hall measurement. Films not undergoing post treatment, however, were the only ones in which field effect could be displayed on the curve tracer; these curves indicated the film may be "n" type.

The heat treatment in air results in a drastic drop in resistance between the source and drain electrodes. For example, one sample read a resistance of 1.8 megohms before air bake, and then dropped rapidly to 16K after the air bake. No explanation will be attempted until more studies are made of these films.

Tin Sulfide

At a boat temperature of 600°C, a film deposition of approximately 100Å/sec occurred. The films studied were 2000Å to 3000Å thick. The films exhibited "p"-type conductivity with a very low Hall-mobility measurement of less than 1 cm^2/volt sec. Field effect was detectable on sensitive test circuits, but so low as not to be able to be displayed on the curve tracer.

2.2 Properties of Semiconductor Films to be Optimized

Tellurium TFTs

Continued improvement in the formation of Te TFTs was achieved this quarter. Evaporations are being carried out in the same general manner as disclosed last quarter, except that a molybdenum boat is being used rather than an intermetallic compound crucible. Reaction between the molybdenum and Te has not been found to be severe. Other heater sources, such as platinum and graphite, were tried, but with lesser success. The Te reacted with platinum and there was inferior results when using a graphite crucible. The importance of a straight metal boat in direct contact to the source (Te) is the closer control of temperature for deposition.

Figure 7 illustrates the characteristics of three Te devices operating at different bias levels and loads. It is obvious that better pinchoff is achieved at lower operating levels. It may be of interest to note the power dissipation of the bottom characteristics of greater than 200 milliwatts.

These devices utilized Te films of approximately 200Å thick and an SiO dielectric of approximately 1500Å. The source-drain electrodes (nichrome 1200Å) are spaced by a 10-micron gap with a length of 100 mils. An aluminum gate of two mils in width completes the device.

Cadmium Selenide and Cadmium Sulfide TFTs

Work was attenuated on devices utilizing these layers this quarter so that other materials might be investigated. Generally, the parameters noted were similar to those reported in the first quarterly report, except that transconductance values have improved by reducing the source-drain spacing to five microns.

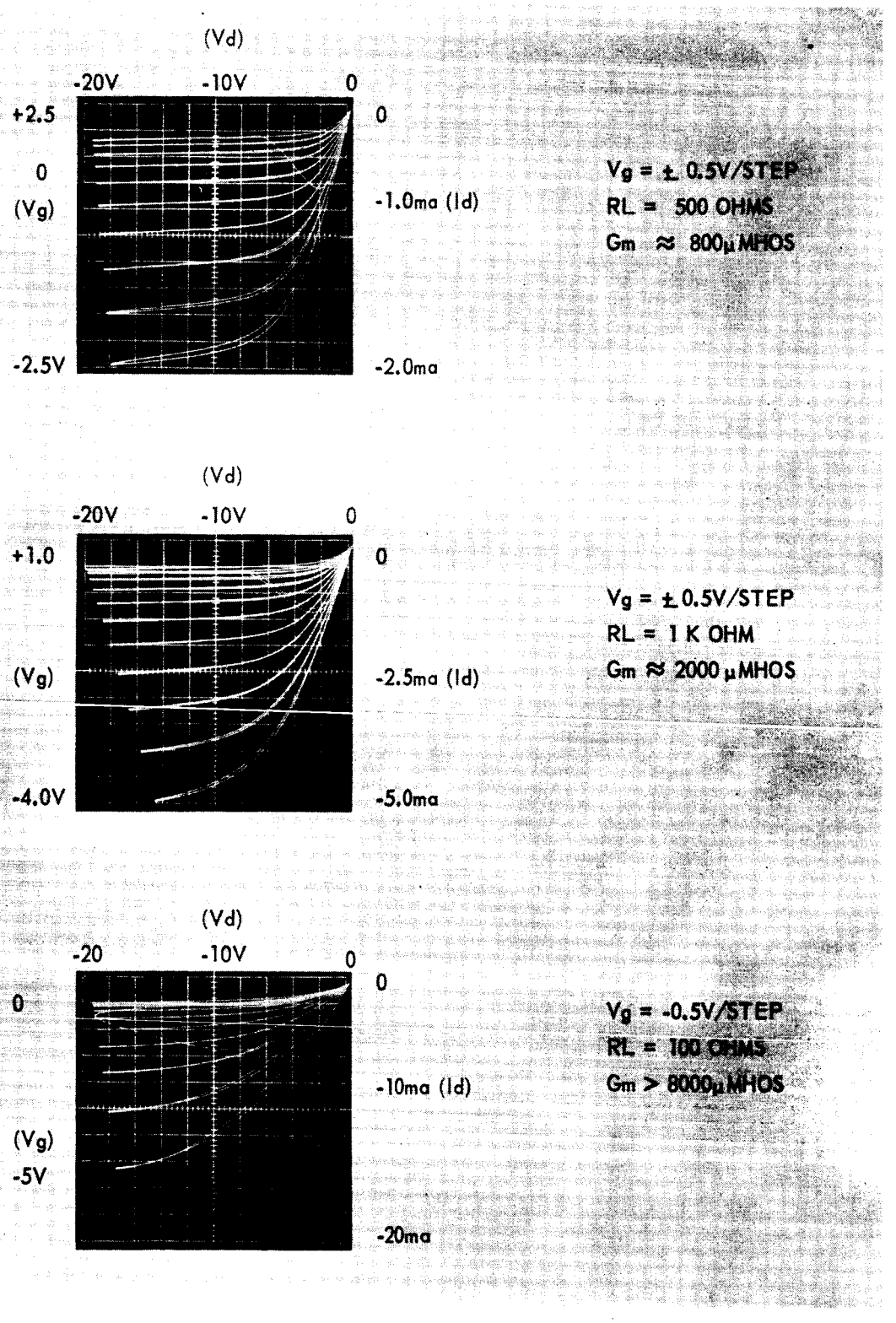

Figure 7. Characteristics of Te TFTs Operated at Different Bias Levels and Loads

Source-drain spacings of 2.5 microns have been formed; the gate electrode width, however, is still a problem area. Thus far, it has been found difficult to make standard etched masks with openings of much less than 0.5 mil and still obtain suitable depositions of this electrode.

At present, nickel-formed masks are being prepared for use in forming narrow gate electrodes. In addition, use of closely spaced wires and other techniques is being investigated.

2.3 Environmental Control

The air-conditioning phase of the "dry room" was completed on June 18, and the relative humidity is now maintained at 25% or below. Some of the work is now being performed in the dry room. Two twin vacuum systems (2-10 in bell jars per system) have been installed as shown in figure 8.

2.4 Field-effect Test Station

A recently fabricated field-effect test station is now in service, as shown in figure 9, and is designed to test TFTs mounted in vacuum cans. The test station will test simultaneously or individually up to 20 devices in either of two modes of operation. The first mode is the application of direct-current potentials to the electrodes of the devices. The drain current and electrode voltages are monitored by panel meters. The second mode of operation is a sweep voltage applied to the source-drain electrodes similar to that of a curve-tracer oscilloscope. The source-gate voltage or "bias" may be independently controlled for each device under test. A type 575 transistor curve tracer is used to monitor the output characteristics of the devices, and may be switched onto individual devices as desired.

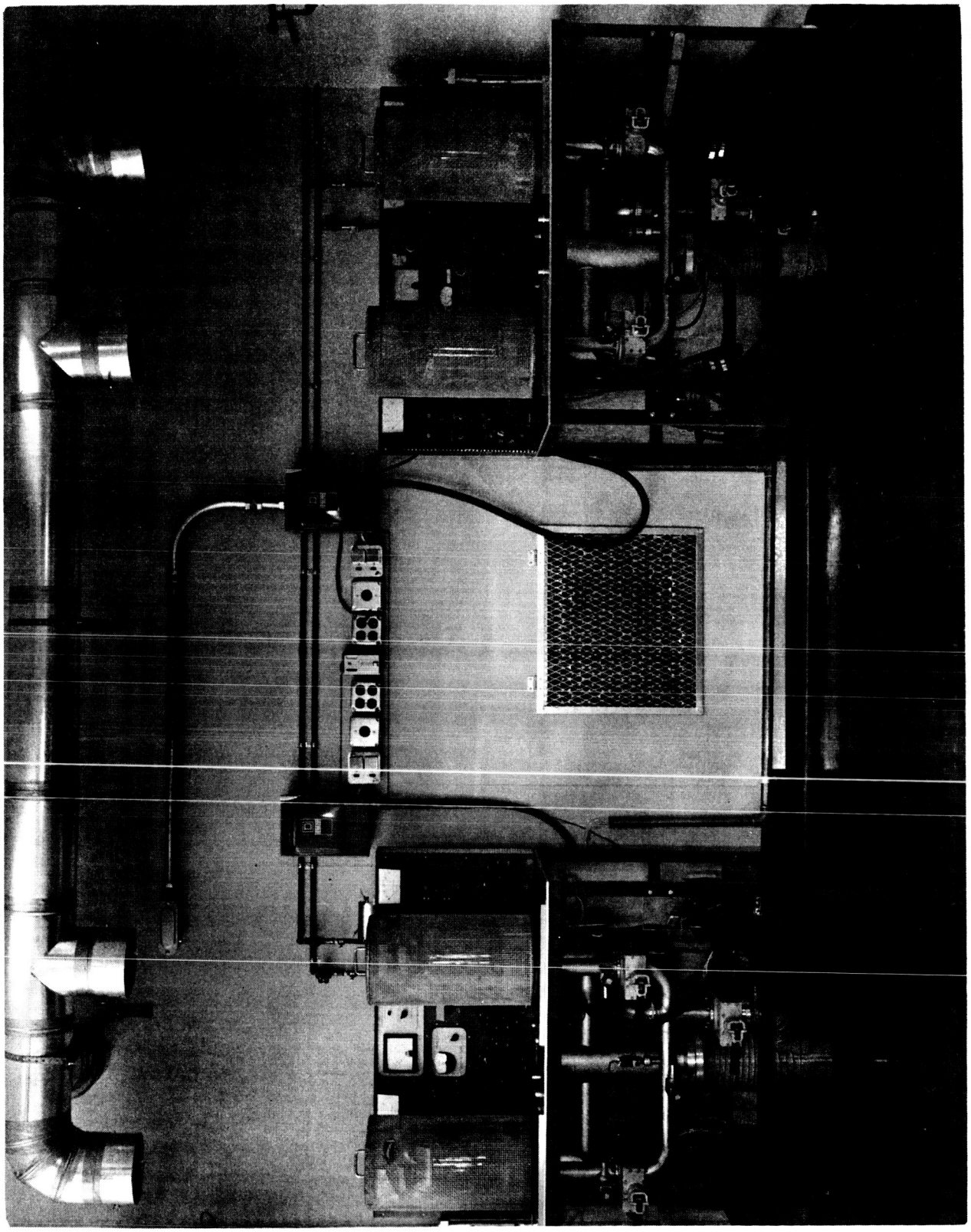

Figure 8. Dual 10-inch Bell Jar Vacuum Systems

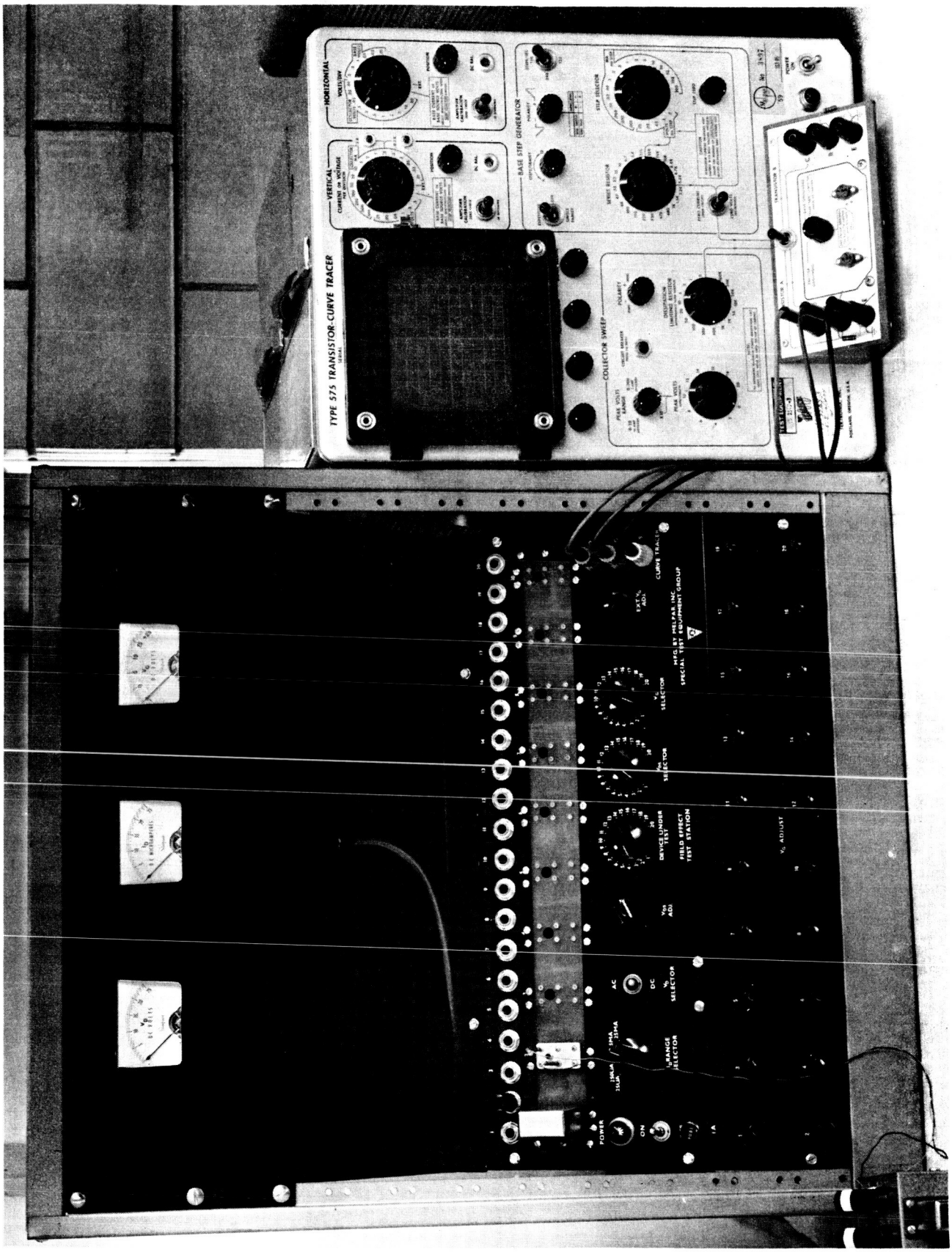

Figure 9. Field-effect Test Station

2.5 Summary

Although field effect was observed in many semiconductor films, the effect was at least an order of magnitude lower than that usually found in properly formed CdSe, CdS, and Te films. Some of these materials show the possibility of being eventually developed into satisfactory field-effect triodes; the effort involved in the optimization of these materials, however, is considered too great at this time. The lack of proper source material is serious, and Melpar must rely upon the chemical industry because most of the materials have not yet been made sufficiently pure.

The most promising of the initially investigated semiconductor materials, CdTe, in conjunction with CdSe, CdS, and Te, will be exclusively and intensively studied. It is the opinion of researchers in this laboratory that these materials, in combination with a suitable device geometry, hold the most promise of fabricating a high-frequency triode in the time allotted for phase A.

3. METAL BASE TRANSISTOR

The work on the metal base transistor has progressed to where work on the emitter (reverse) junction is ready to be initiated. A preliminary investigation has shown that "reverse" junctions can be formed by depositing CdSe and ZnSe simultaneously from two separate crucibles. The deposition temperatures for fabricating the reverse junction are such that they will not change the characteristics of the first junction. This was verified by subjecting several collector junctions to heating cycles, in the vacuum, at temperatures in excess of the anticipated reverse junction substrate temperatures. All the junctions exhibited the same characteristics before and after the test. Because of these results, 48 collector junctions were successfully fabricated for incorporation into the complete metal base structure. During this work, however, it was noted that the use of ZnSe materials from different suppliers resulted in junctions of widely varying properties. Therefore, a major portion of the effort this quarter was directed toward the evaluation of these materials.

3.1 Materials Evaluation

A supply of ZnSe material from Penn Rare Metals, Inc., Metal Hydrides, Harshaw Chemical Company, and Kern Chemical Corporation has been investigated. The evaluation of these materials was performed by comparing the characteristics of the junctions formed by depositing mixtures of these various ZnSe materials with CdSe from L. Light and Company.

Because the properties of the various ZnSe materials varied somewhat, an "optimum" set of deposition parameters was found for each material, and

the evaluation was based on junctions formed by "optimum," rather than identical, deposition conditions. At least 80 junctions were fabricated from each ZnSe material. The I-V characteristics of a typical junction formed from each one of the ZnSe materials are shown in figure 10.

Figure 10a shows the characteristics of a junction formed by using ZnSe from Penn Rare Metals, Inc. These junctions are easily reproduced and exhibit the following typical properties: reverse breakdown voltage = 8-10 volts; forward breakdown voltage = 0.3-0.6 volts; static rectification ratio = 10^4 -10^5 at 0.8 volts; leakage current $\leq$1μa at a reverse bias of 4 volts; and forward resistance $\leq$ 100 ohms. These junctions also exhibit excellent shelf life and operational stability at room ambient.

Figure 10b shows the characteristics of a junction formed by using ZnSe from Metal Hydrides, Inc. These junctions are very difficult to reproduce and exhibit the following typical properties: reverse breakdown voltage = 5-6 volts; forward breakdown voltage = 2-3 volts; static rectification ratio = 10^4 at 3 volts; leakage current $\simeq$1μa at a reverse bias of 4 volts; and forward resistance $\leq$ 500 ohms. These junctions exhibit good shelf-life stability, but their operation is characterized by a slow response to applied voltage. This is indicative of a large concentration of deep trapping levels.

Figure 10c shows the characteristics of a junction formed by using ZnSe from Harshaw Chemical Company. These junctions are fairly difficult to reproduce and exhibit the following typical properties: reverse breakdown voltage = 3-4.5 volts; forward breakdown voltage = 0.4-0.8 volts; static rectification ratio = 10^4 at 1 volt; leakage current $\simeq$2μa at a reverse bias

SCALE:
- FORWARD BIAS: 0.5MA/DIV - VERTICAL; 1V/DIV - HORIZONTAL
- REVERSE BIAS: 0.01MA/DIV - VERTICAL; 1V/DIV - HORIZONTAL

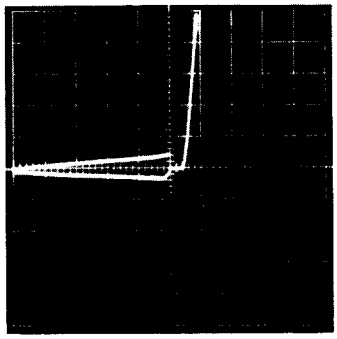

(a) PENN RARE METALS INC.

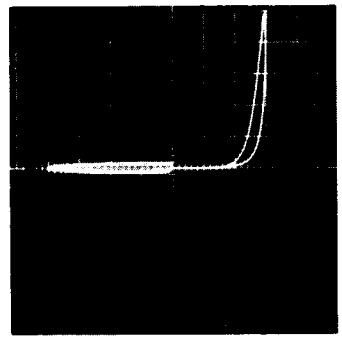

(b) METAL HYDRIDES

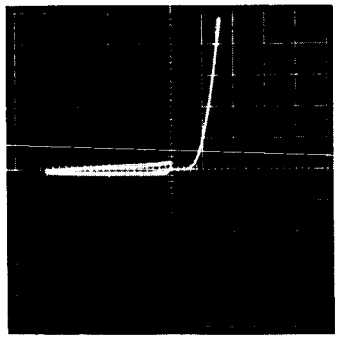

(c) HARSHAW CHEMICAL CO.

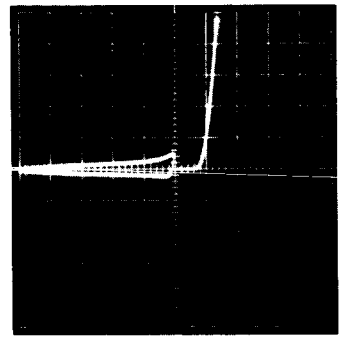

(d) KERN CHEMICAL CORP.

Figure 10. Characteristics of CdSe-ZnSe Rectifiers Using ZnSe From Different Suppliers

of 4 volts; and forward resistance $\leq$ 500 ohms. These junctions exhibit excellent shelf life and operational stability at room ambient.

Figure 10d shows the characteristics of a junction formed by using ZnSe from Kern Chemical Corporation. These junctions are presently being investigated and indicate that they are fairly easy to reproduce. Some junctions formed from this material exhibit the following properties: reverse breakdown voltage = 6 volts; forward breakdown voltage = 0.3-0.8 volts; static rectification ratio = 10^4-10^5 at 1 volt; leakage current $\leq$ 1μa at a reverse bias of 4 volts; and forward resistance $\leq$ 200 ohms. The deposition parameters for these junctions are still being optimized.

The materials investigation has shown that ZnSe from Penn Rare Metals, Inc., is compatible with CdSe from L. Light and Company for forming transistor quality junctions. Preliminary studies indicate that ZnSe material from Kern Chemical Corp. will also be suitable.

ZnSe from Harshaw Chemical Company forms junctions with relatively low reverse breakdown voltages. Junction parameters are also fairly difficult to reproduce. ZnSe from Metal Hydrides, Inc., forms junctions with relatively low reverse and forward breakdown voltages. Along with being very difficult to reproduce, these junctions also indicate the presence of deep trapping levels. Therefore, materials from these suppliers are judged unsuitable. It is noted, however, that these materials might be compatible with CdSe from a different supplier for forming junctions with desirable properties. No effort will be directed toward this investigation.

3.2 Junction-stability Investigation

Seventy-five junctions are presently being shelf-life tested. These junctions were formed from Penn Rare Metals, Inc., ZnSe. The junctions are unprotected, and are stored at normal ambient conditions. After 2500 hours, there have been no junction failures and their I-V characteristics have remained stable within experimental error.

Five junctions were operated continuously at room ambient. After 120 hours, no change was noted in their I-V characteristics. These five junctions were then returned to shelf-life testing after the 120 hours of continuous operation. To date, no change in parameters has been observed in any of the junctions.

3.3 Temperature Dependence of Junction Parameters

The temperature dependence of the junction parameters was of interest for two specific reasons: (1) to aid in the determination of the operational mechanism and (2) to determine whether the junctions could withstand the temperatures required for the fabrication of the reverse junction.

Figure 11 shows the reverse and forward bias temperature behavior of a CdSe-ZnSe rectifier (ZnSe from Penn Rare Metals, Inc., was used to form this junction). This sample was heat cycled in the vacuum at a pressure of about 10^{-7} mm Hg and was kept at each temperature for approximately one-half hour to attain equilibrium. The sample was then stored for one hour at 160°C. During this entire test, the sample was being continuously operated.

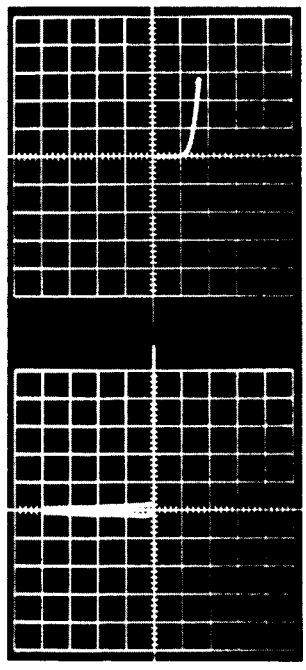

0.2MA/DIV - VERTICAL
0.5V/DIV - HORIZONTAL

0.01MA/DIV - VERTICAL
1V/DIV - HORIZONTAL

(a) 25°C

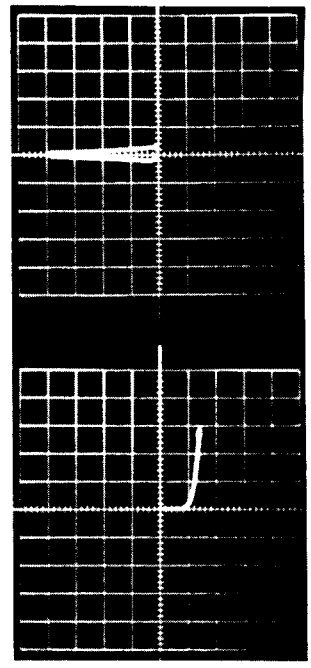

0.01MA/DIV
1V/DIV

0.2MA/DIV
0.5V/DIV

(b) 46°C

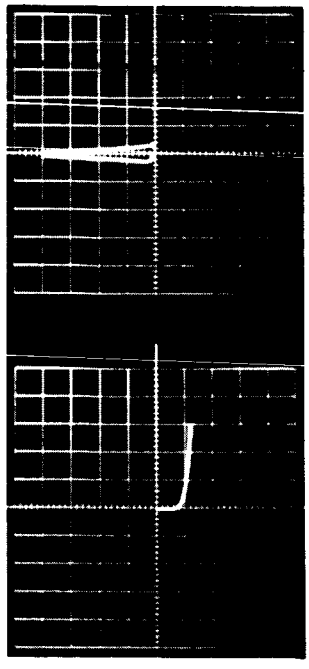

0.01MA/DIV
1V/DIV

0.2MA/DIV
0.5V/DIV

(c) 60°C

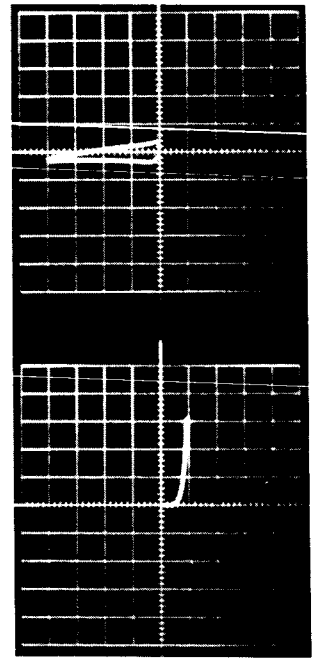

0.01MA/DIV
1V/DIV

0.2MA/DIV
0.5V/DIV

(d) 90°C

Figure 11. Variation of Junction Parameters with Temperature (Sheet 1 of 2)

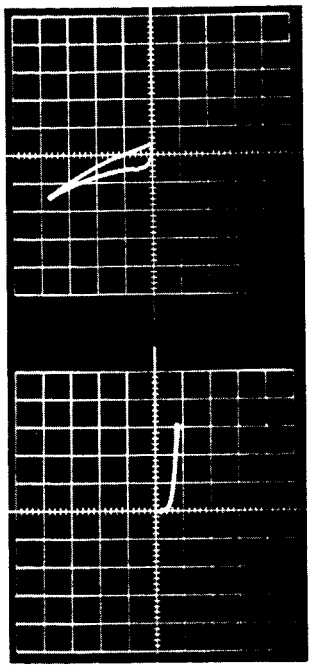

0.01 MA/DIV
1V/DIV

0.2MA/DIV
0.5V/DIV

(e) 106°C

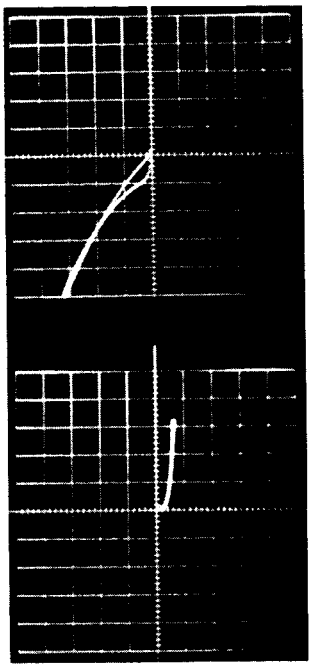

0.01MA/DIV
1V/DIV

0.2MA/DIV
0.5V/DIV

(f) 128°C

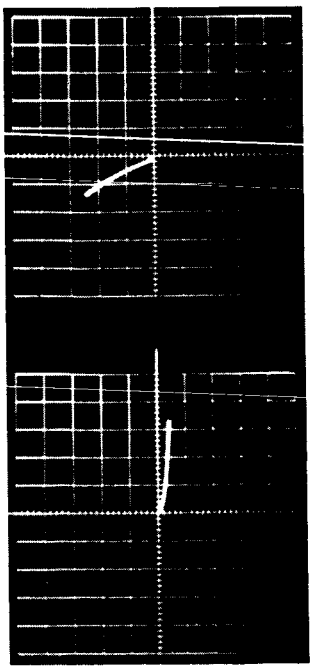

0.2MA/DIV
1V/DIV

0.2MA/DIV
0.5V/DIV

(g) 160°C

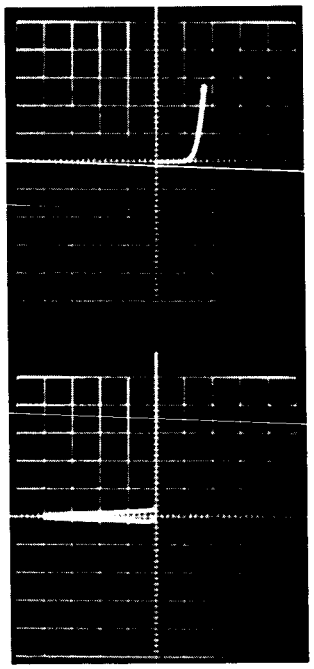

0.2MA/DIV
0.5V/DIV

0.01MA/DIV
1V/DIV

(h) 25°C END OF CYCLE

Figure 11. Variation of Junction Parameters with Temperature
(Sheet 2 of 2)

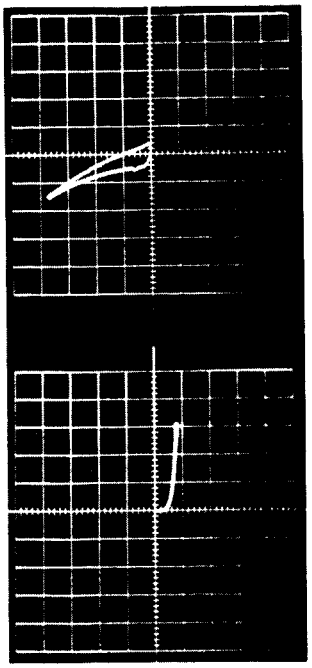

0.01 MA/DIV
1V/DIV

0.2MA/DIV
0.5V/DIV

(e) 106°C

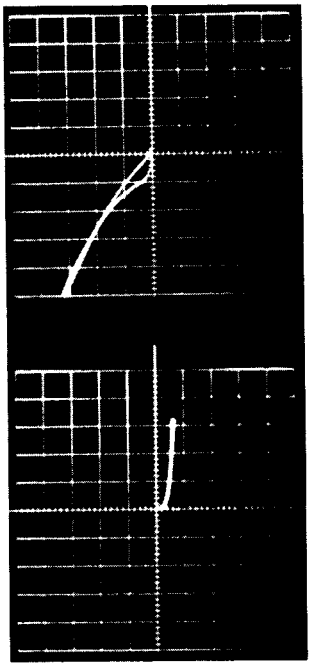

0.01MA/DIV
1V/DIV

0.2MA/DIV
0.5V/DIV

(f) 128°C

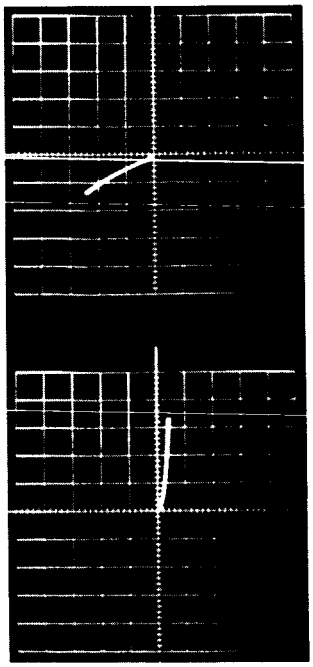

0.2MA/DIV
1V/DIV

0.2MA/DIV
0.5V/DIV

(g) 160°C

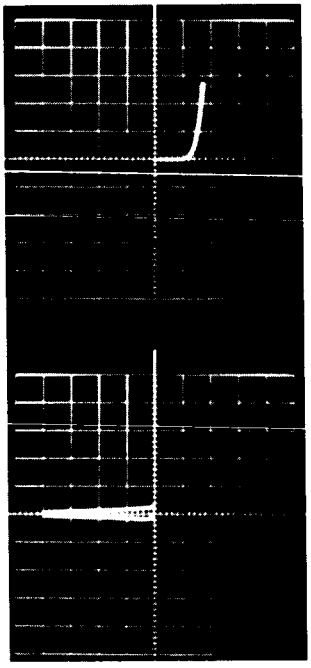

0.2MA/DIV
0.5V/DIV

0.01MA/DIV
1V/DIV

(h) 25°C END OF CYCLE

Figure 11. Variation of Junction Parameters with Temperature
(Sheet 2 of 2)

The variation with temperature of the leakage current and the forward breakdown voltage are given in table I.

A significant result of this test is the reversibility of the junction parameters with temperature. Storage in vacuum for one hour at 160°C caused no permanent damages or changes. A comparison between figures 11a and 11h shows the junction parameters to be identical before and after the heat cycle. The ability of the junction to withstand storage in vacuum at 160°C without change makes it compatible with the anticipated fabrication temperatures of the reverse junction.

Table I

VARIATION OF JUNCTION PARAMETERS WITH TEMPERATURE

Temperature (°C)	Leakage current at eV (μa)	Forward breakdown voltage (Volts)
25	<1	0.60
46	<1	0.50
60	≈1	0.45
90	2	0.30
106	11	0.25
128	46	0.15
160	400	0.05

4. DIELECTRIC INVESTIGATION

In the First Quarterly Report, it was shown that capacitors at high frequencies could behave like inductors if their geometry is not taken into consideration. For the borosilicate dielectric film, the transition length between capacitive and inductive behavior (transmission-line length of $\frac{\lambda g}{4}$ for 300 mc) of thin-film capacitors was found to be approximately 12 centimeters. Thus, at least theoretically, a thin-film capacitor should provide capacitive reactance up to 300 mc for all lengths up to 12 centimeters. The area of a capacitor is a factor to be considered in the design of capacitors of specific capacitance values. For large values of capacitance, where capacitor length approaches the quarter wavelength of the equivalent transmission line, the geometry must be considered with respect to the length-to-width ratio and the connection point of the leads. Rectangular capacitors with dimensions of 12 cm x 6 cm would have a higher upper-frequency limit if the leads were placed on the long side of the plates so that the length is 6 cm and the width 12 cm. This has been shown by Dukes.[2] Because thin-film capacitors will be much less than 12 cm in length, however, these critical geometry considerations are not considered to be necessary for operation up to 300 mc.

4.1 Capacitor-frequency Measurements

The fabrication and testing of high-frequency capacitors were undertaken this quarter. Capacitors were fabricated with both SiO and borosilicate dielectrics in the production evaporation system. The capacitor plates were evaporated aluminum. These capacitors had values of 80 and 120 pf respectively.

The anticipated method of evaluating these capacitors was by using the Boonton, 190A, Q meter. This instrument was found, however, to be unsatisfactory for making capacitance measurements by either parallel or series techniques above 70 megacycles. Thin-film capacitors as well as commercial high-frequency silver/mica capacitors deviated drastically from their expected values above this frequency. The apparent capacitance for both types of capacitors increased rapidly with frequency until the reactance eventually appeared inductive to the Q meter. This deviation from the expected behavior for standard high-frequency capacitors indicated that, at frequencies above about 70 mc (the upper-frequency limit depends on the value of capacitance), the Q meter was incapable of accurate capacitance measurement for these values of capacitance. Below 70 mc, the Q meter gives an accurate representation of capacitor behavior.

As an alternative approach to this problem, the circuit in figure 12 was employed. The marker generator is a Hewlett-Packard, model 608-D, VHF signal generator. The sweep-frequency generator is a Jerrold, model 900A, using a model D-50 detector, and the display is shown on a Tektronix, type 541, oscilloscope with a type 53-B plug-in unit. The sample is connected between the sweep output of the sweep-frequency generator and the detector. The voltage at the detector is displayed on the vertical axis of the oscilloscope. The resulting "blips" correspond to the primary subharmonics and harmonics of the marker frequency and, thus, give frequency reference points on the oscilloscope sweep.

When a shorting bar (1.0" X 0.4" X 0.010" platinum sheet) is placed between the sweep output and the detector, the voltage output from these

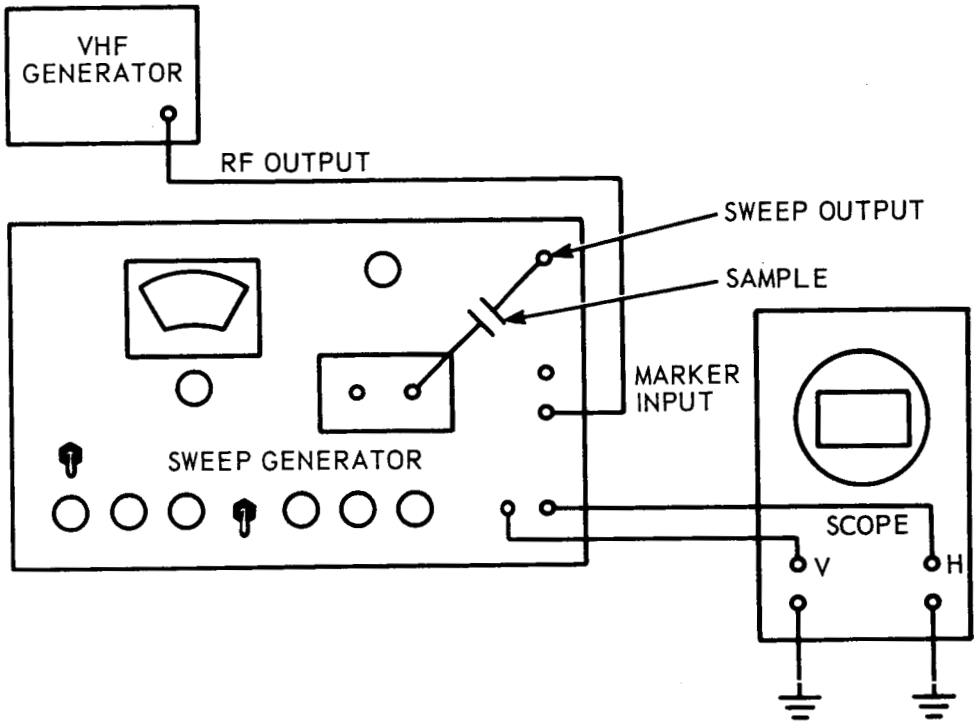

Figure 12. Block Diagram of High-frequency Capacitor Evaluation Equipment

terminals is displayed directly as a function of frequency on the oscilloscope. This display is shown in figure 13a. The bandwidth of the sweep is from 0.1 mc to 400 mc with the 200-mc marker "blip" shown at 5.8 centimeters. The subharmonic corresponding to 100 mc is shown at 2.8 centimeters, the 300-mc harmonic is partially concealed at 8.3 centimeters, and the 400-mc marker is shown at the end of the trace near 9.9 centimeters. A similar oscilloscope display with the shorting bar replaced by a thin-film borosilicate capacitor (120 pf) is shown in figure 13b. Note that from approximately 50 mc the capacitor behaves like a short circuit to alternating current all the way to 400 mc. This is an indication of excellent capacitor performance. Figure 14 (a and b) shows similar photographs of oscilloscope displays with the platinum shorting bar and a thin-film SiO capacitor respectively connected to the sweep generator. The bandwidth is again 0.1 mc to 400 mc, with markers faintly located at 100 mc (3.2 cm), 200 mc (5.6 cm), 300 mc (7.6 cm), and 400 mc (9.9 cm).

Figure 15 (a and b) shows oscilloscope displays with the shorting bar and a standard 100-pf mica capacitor respectively connected to the sweep generator. The bandwidth here is 0.1 to 430 mc, with markers at 50 mc (1.3 cm), 100 mc (2.5 cm), 200 mc (5.1 cm), 300 mc (7.1 cm), and 400 mc (9.3 cm).

4.2 Conclusions

The results of the study indicate that the thin-film capacitors behave as well as standard, commercially available, high-frequency capacitors at high frequencies and there should be absolutely no problem with thin-film

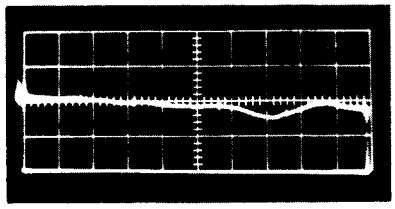

HORIZONTAL: 0.1 TO 400MC

VERTICAL: 0.2 VOLTS/CM

a

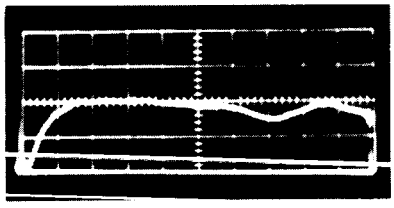

HORIZONTAL: 0.1 TO 400 MC

VERTICAL: 0.2 VOLTS/CM

b

Figure 13. Oscilloscope Display of AC Voltage Passed as Function of Frequency by (a) Shorting Bar and (b) Thin-film Borosilicate Capacitor

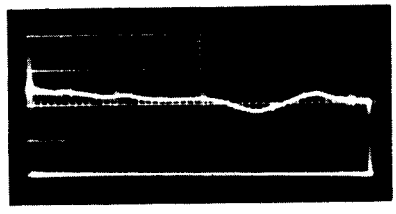

HORIZONTAL: 0.1 TO 400MC

VERTICAL: 0.2 VOLTS/CM

a.

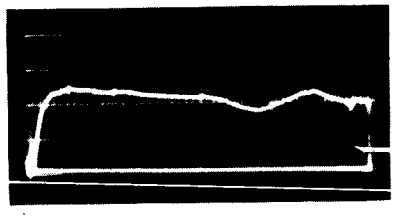

HORIZONTAL: 0.1 TO 400MC

VERTICAL: 0.2 VOLTS/CM

b.

Figure 14. Oscilloscope Display of AC Voltage Passed as Function of Frequency by (a) Shorting Bar and (b) Thin-film SiO Capacitor

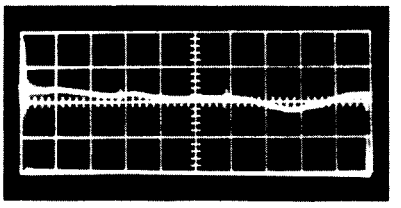

HORIZONTAL: f = 0.1 TO 400MC

VERTICAL: V = 0.2 VOLTS/CM

a

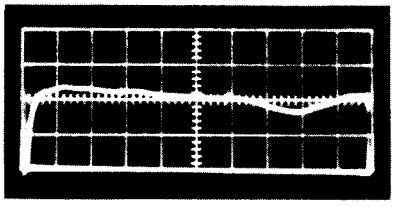

HORIZONTAL: f = 0.1 TO 400MC

VERTICAL: V = 0.2 VOLTS/CM

b

Figure 15. Oscilloscope Display of AC Voltage Passed as Function of Frequency by (a) Shorting Bar and (b) High-frequency Standard Silver/Mica Capacitor

capacitor operation at frequencies up to 400 mc. The low-frequency cutoff seen for all capacitors is an indication that the capacitors are not shorted and that they are blocking low-frequency a-c voltage. Larger-valued capacitors would extend this cutoff to still lower frequencies. There is no detectable difference in the frequency behavior between SiO and the borosilicate thin-film capacitors in this frequency range. The borosilicate thin-film capacitors are preferred, however, over the SiO capacitors because of their higher d-c resistance, higher dielectric breakdown strength, and better temperature stability.

5. INDUCTORS

5.1 General

Table II gives the inductance and associated equations that have been used in this program. Some of the equations have been modified by the experimental results achieved at this facility, as explained in the notes.

The purpose of this inductor investigation has been to determine the feasibility of using thin-film inductors. This means achieving usable Q values at the desired frequencies. Also, the values of inductance at low frequencies must be large enough to ensure the use of reasonably-sized capacitors.

5.2 Frequency

The problems of forming a useful inductor are different at the frequency extremes and, therefore, are divided into two sections.

5.2.1 High Frequency

The limiting factor for a high-frequency inductor is the length of conductor that forms the coil. Combining equations (4) and (5), using 300 megacycles per second for f_o (actual) and solving for the conductor length (ℓ), yields a maximum conductor length of 3.24 inches for an actual self-resonant frequency at 300 megacycles per second. Therefore, to use a thin-film inductor at 300 megacycles per second, the conductor length must be less than 3.24 inches (2.44 inches for an f_o (actual) of 400 mcps). This length is the limiting factor on the inductance that can be achieved at high frequencies.

Table II

INDUCTANCE EQUATIONS

(All equations refer to figure 16)

a) Flat, spiraling, square coils; general

$$L = 0.141\, an^{5/3} \log 8\,\frac{a}{c} \text{ (microhenries)} \quad (1)$$

$$a = \frac{A + B}{4} \text{ (inches)}$$

$$c = \frac{A - B}{2} \text{ (inches).}$$

(or combined)

$$L = 0.035(A+B)n^{5/3} \log \left(4\,\frac{A+B}{A-B}\right) \text{ (microhenries)} \quad (1)$$

$$L \text{ (actual)} = 1.28L \text{ (equation 1)} \quad (2)$$

$$L_T = L_1 + L_2 + K\sqrt{L_1 L_2} \quad (3)$$

$$f_o \text{ (theoretical)} = \frac{c}{4\ell\sqrt{\varepsilon_r}}\ \frac{0.148\times10^{10}}{\ell} \text{ (cycles per second} \quad (4)$$

$$f_o \text{ (actual)} = 0.66 f_o \text{ (theoretical)} \quad (5)$$

$$f = \frac{1}{2\pi\sqrt{LC}} \quad (6)$$

$$Q = \frac{2\pi fL}{R_{coil}} \quad (7)$$

$$d = \frac{1}{\sqrt{\pi f \mu\sigma}} \text{(meters)} = \frac{6.61\times10^{8}}{\sqrt{f}} \text{ angstroms (copper)} \quad (8)$$

b) Flat, spiraling, square coils; with inner diameter equal to zero

$$L = 0.210\, An^{5/3} \text{ (microhenries)} \quad (9)$$

$$n = \frac{A}{2(x+y)} \text{ (turns)} \quad (10)$$

$$\ell = 2\,An \text{ inches} \quad (11)$$

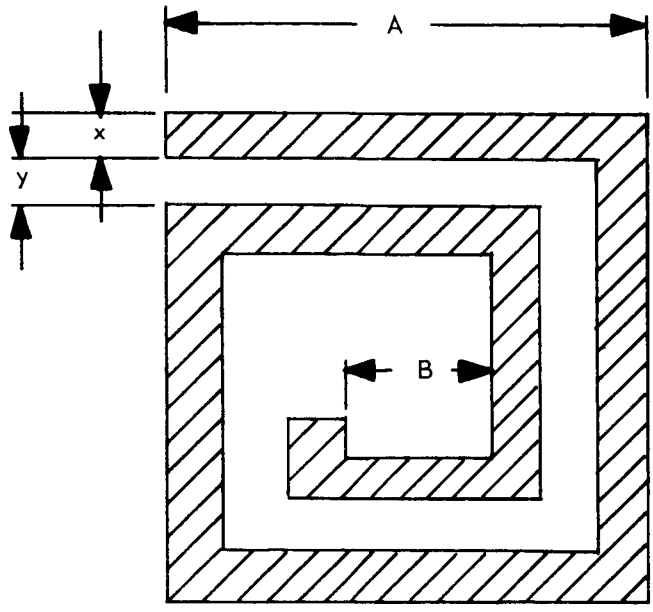

A = OUTER "DIAMETER"
B = INNER "DIAMETER"
x = CONDUCTOR WIDTH
y = SPACING BETWEEN CONDUCTORS
N = NUMBER OF TURNS
L = LENGTH OF CONDUCTOR IN COIL

Figure 16. Thin-film, Flat, Square Spiraling Inductor

c) Definition of terms

A = outer "diameter" (inches)

B = inner "diameter" (inches)

n = number of turns in coil

L_T = total inductance

K = mutual inductance coupling coefficient

f_o = self-resonant frequency of coil (cycles per second)

c = velocity of light in free space (inches per second)

ℓ = length of conductor in coil (inches)

f = frequency (cycles per second)

L = inductance (microhenries everywhere except henries in equation 6)

C = capitance (Farads)

ε_r = substrate dielectric constant

R_{coil} = total resistance of coil (ohms)

d = skin depth (meters)

μ = permeability (henry per meter)

σ = conductivity (mho per meter)

x = conductor width (inches)

y = spacing between conductors (inches)

d) References

Equation 1; reference 3.

Equation 4; reference 2.

Equation 8; reference 4.

Equation 10; reference 5.

Equation 11; reference 5.

e) Notes

Equation 1 is an empirical formula developed by Bryan[3] for printed-circuit inductors. The results of forming coils, in the First Quarterly Report, show that this equation was valid for the larger-spaced inductors. However, when forming inductors using 10-mil lines and 10-mil spacing (figure 17), equation 2 gives the corrected empirical inductance equation.

Also shown in the First Quarterly Report is the derivation of a mean "velocity factor" from the experimental results. This "velocity factor" of 0.66 is used to form equation 5.

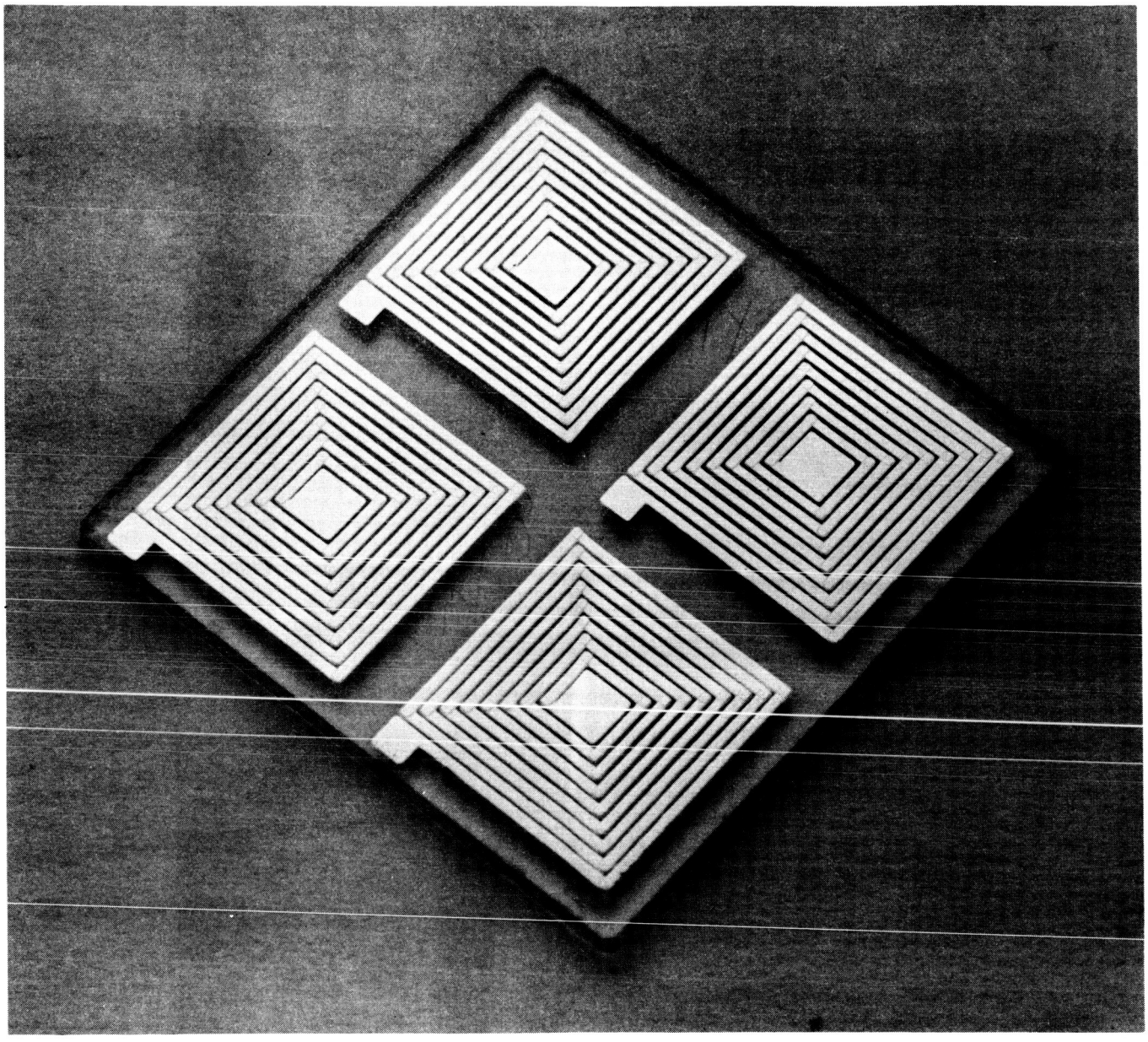

Outer diameter = 0.4 inches
Conductor width = 0.010 inches (10 mils)
Spacing between conductors = 0.010 inches (10 mils)
Inductance = 0.5 microhenries
Q at 30 megacycles = 10

Figure 17. Thin-film Inductors (Completely Vacuum Deposited)

For example, a one-turn coil with an outer diameter (A) of 0.6 inch and an inner diameter (B) of 0.5 inch would be 2.4 inches long if the square loop were closed. Obviously, it will be slightly shorter so that the loop will be open and connections can be made. Using equation (1), this results in an inductance of 0.064 microhenry. If the conductor width is 50 mils, using a length of 2.4 inches results in a conductor of 48 squares. At a resistance of 0.01 ohm per square, the d-c resistance of the coil will be 0.48 ohm. If the d-c resistance is used for the high frequencies (this will not be true because of the skin effect) just for comparison, the Q of the coil at 300 megacycles per second is 252 (equation 7). More important, the capacitance necessary for tank circuit resonance at 300 megacycles is only 4.4 picofarads (equation 6). This capacitance is so small that it would be desirable to actually decrease the inductance for use at 300 megacycles.

This same inductor can be examined at lower frequencies. If the d-c resistance is again used for comparison only, solving equation (7), using 0.064 microhenry, the resistance of 0.48 ohm and a Q value of 10, will result in a frequency of 12 megacycles. This means that, at 12 megacycles, this coil has a Q of 10 and will resonate in a tank circuit at this frequency with a capacitance value of 2750 picofarads (equation 6). There is no problem involved in achieving more than 10,000 picofarads per square centimeter in thin-film form. Therefore, this inductor could be used at lower frequencies, particularly if capacitor trimming were desired for precise tank-resonant frequencies.

5.2.2 Lower Frequencies

At lower frequencies, approximately 30 megacycles, the inductor coil length is a limiting factor, not because of self-resonance, but because of the added coil resistance which limits the attainable Q values. It is possible to obtain four times the inductance of a coil by using two coils in series aiding and having them mutually couple each other with a coupling factor of one. This is shown in equation 3. The resultant four times the inductance value coupled with only twice the resistance values (two coils) should result in a doubled Q factor at any frequency (equation 7). Therefore, the same inductors discussed in the First Quarterly Report were deposited in an effort to achieve the parameters discussed above.

The results are shown in table III. The coils deposited on quartz substrates without any other depositions were reported in the First Quarterly Report; they are repeated here in numbers 1, 2, and 3. Numbers 1A, 2A and 3A are coils deposited on opposite sides of quartz substrates which are 40 mils thick and connected through the center of the substrate in series aiding. The results are compared with four times the inductance and one-half the self-resonant frequency actually obtained with single coils listed under numbers 1, 2, and 3. The inductance values and self-resonant frequencies actually obtained could all be considered "ball park" figures when compared with the expected values. There was, however, no improvement in Q value, which was expected to double. As a check on the experiment, the two coils were separated and the single-coil measurements are presented under numbers 1B, 2B, and 3B. These values (1B, 2B, and 3B) differ from

Table III

INDUCTOR VALUES

Substrate	Conductor width (mils)	Space (mils)	Outer diameter (mils)	Inner diameter (mils)
1	25	25	0.8	0
2	35	15	0.8	0
3	15	35	0.8	0

Substrate	Theoretical L(μh)	Theoretical f_o(mc)	Actual L(μh)	Actual f_o(mc)	Q (30mc)
1	0.544	105	0.602	74.7	11.5
2	0.544	105	0.569	76.9	12
3	0.544	105	0.664	71.7	9.2

Substrate	Expected L(μh)	Expected f_o(mc)	Q (30mc)	Actual L(μh)	Actual f_o(mc)	Q (30mc)
1A	2.41	37.35	23	2.64	35	9.1
2A	2.28	38.45	24	2.74	34	7.9
3A	2.66	30.85	18.4	3.17	33.3	8.1

Substrate	Expected L(μh)	Expected f_o(mc)	Q (30mc)	Actual L(μh)	Actual f_o(mc)	Q (30mc)
1B	0.602	74.7	11.5	0.675	61	10.1
2B	0.569	76.9	12	0.625	62	9.2
3B	0.664	71.7	9.2	0.742	60.2	8

Notes:

1. Englehard quartz substrates (one inch square and 40 mils thick).
2. All values measured at 30 mc.

their counterparts (1, 2, and 3) by having slightly higher inductance with slightly lower self-resonant frequencies and Q values. This can be explained by the fact that there is a metal deposition on the other side of the substrate (the other coil), and this should affect the measured coil in the manner noted above. The unexplained question is "Why didn't the Q factor, if not double, at least increase?" The immediate observation is that the losses incurred in the mutual coupling through the quartz medium are lowering the Q. This theory seems logical when the actual definition for the "quality factor" is used.

$$Q = \frac{2\pi \text{ total energy stored}}{\text{energy dissipated per cycle}}$$

Therefore, any added losses, which could be in the coupling, would tend to decrease the Q value. It also should be noted here that attempts to stack coils in series aiding, separating them with 20,000 angstroms of silicon monoxide, were not successful since the inductive effects were swamped out by the capacitance between the coils.

The substrates with coils on either side, however, demonstrate sufficient coupling to warrant further investigation for possible low-power transformer applications.

5.3 Resistivity

The importance of the "skin depth" phenomenon of increasing the film resistance as a function of frequency was presented in the First Quarterly Report. The calculated part of equation 8 holds true only as long as the conductivity and permeability of the thin film of copper are the same as the bulk values. The resistivity (the reciprocal of the conductivity) of

copper films at least 10,000 angstroms thick has been found to equal bulk resistivity. The minimum thickness for which the resistivity of copper films drops to bulk value is probably about 2000 angstroms. All conductor films used in formation of inductors, however, should be at least 17,240 angstroms thick since this is the thickness required to obtain a sheet resistance not greater than 0.01 ohm per square. This value is necessary to obtain fairly reasonable Q values. The resistivity is related to film thickness in the following manner:

$\rho = 0.01\ R'd$

ρ = resistivity (microhm-cm)

R' = sheet resistance (ohms per square)

d = film thickness (angstroms)

Since the films are thick enough to have bulk resistivity, it is assumed that they also have bulk permeability; therefore, bulk values are used in the calculations concerning skin depth.

5.4 Conclusions

Stress was placed this quarter on attempting to increase the inductance per unit area, and in the evaluation of commercial inductors so that the feasibility of thin-film inductors could be more realistically ascertained. The results were that the commercial inductors for frequencies around 300 megacycles per second were on the order of 0.05 microhenry, just as the thin-film inductors. The attempt at increasing the inductance and Q by stacking inductors was only partially successful. Sufficient coupling was obtained, however, to encourage further investigation of isolation coupling of low-power signals.

Next quarter, work will be done on forming small-value inductors for use at high frequencies. The masks are now being fabricated. These inductors can be used at lower frequencies because the short length of conductor forming the coil results in very low total resistance, which will result in usable Q values. These coils are being formed with various conductor widths so that the actual a-c resistances as a function of conductor width can be studied.

6. HIGH-PERMEABILITY FERRITE FILMS

6.1 Introduction

The methods of vacuum depositing ferrite films were described in the First Quarterly Report. The techniques developed during that period have been proven successful, and no notable changes were incorporated.

The investigations of thin ferrite films are progressing satisfactorily. The results achieved, however, during the past quarter have not yet been translated to the practical stage of inductor formation and evaluation. The fabrication of the magnetic drive and sense coils, as well as the assembly of the electronic equipment, proved to be a series of exacting tasks. These results are explained more fully in this section.

6.2 Physical Characteristics of Ferrite Films

6.2.1 Fe_3O_4-B_2O_3 Mixtures

6.2.1.1 Chemical Composition and Film Structure: The series of Fe_3O_4-B_2O_3 mixtures ranges from 100% to 90% of Fe_3O_4 to 0-10% B_2O_3 by weight were deposited from tungsten boats. A total of 106 films was deposited, and the general appearance of the films can be related to initial mixtures. The films formed from the 100% Fe_3O_4 exhibited a metallic luster, and material decomposition had occurred. Films from a 99% Fe_3O_4 - 1% B_2O_3 mixture showed a lesser degree of metallic appearances. The 95% Fe_3O_4 - 5% B_2O_3 and 90% Fe_3O_4 - 10% B_2O_3 mixtures resulted in films that were dark and exhibited the ferrite structures as described in the First Quarterly Report. The degree of film crystallinity increased with high substrate temperatures. The maximum substrate temperature was 750°C.

Because it was possible that the magnetic properties of the films may be due to free or elemental Fe (the reduced state of Fe_3O_4) in the film, a 95% Fe_3O_4 - 5% B_2O_3 film was chemically analyzed for Fe content. The standard technique, which is sensitive, was employed. The film on the fused silica substrate was immersed in a solution of ferric chloride solution for three days. The purpose was that the ferric chloride would oxidize to ferrous chloride. Thus, by calibrating a standard solution by means of titrating the ferrous chloride, the amount of free iron can be determined. The measured value of the ferrite films was less than 100 ppm, which was the minimum detectable limit of the calibrated solution. These results, although not comprehensive, verify the previous findings.

6.2.1.2 Optical Reflectance Spectra: The film's structure was studied by means of optical reflectance spectra from 2000 Å to 15-microns wavelength. The films were analyzed respectively on a Cary 15 spectrophotometer and a Beckman IR 5A spectrophotometer. The results are shown in figures 18 and 19 for the visible and infrared regions. The smooth line curve in figure 18 is the reflectance curve of bulk Fe_3O_4 obtained by Vratny and Kokalas.[6] On the same tracing is the reflectance curve obtained from the vacuum-deposited ferrite films. The bands at 390 mμ and 580 mμ show good agreement. The band at 510 mμ of the bulk sample does not have an exact agreement with the film; the band in the film appears at about 530 mμ rather than 510 mμ. The reflectance spectra of the ferrite film in the infrared region (2-15μ) show structure and a strong absorption peak at 2.7μ with other less pronounced peaks at 3.7μ, 4.15μ, and 4.85μ. The data presented in the infrared region

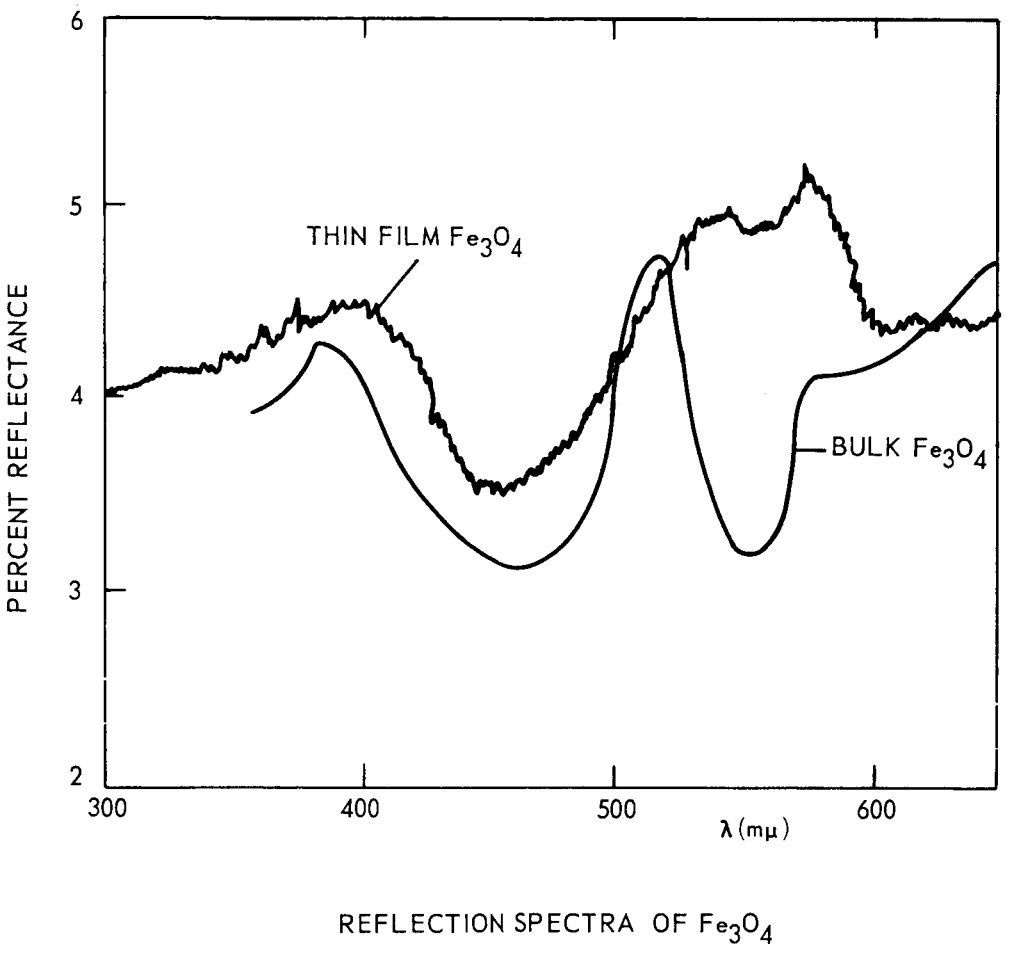

Figure 18. Reflection Spectra of Fe_3O_4

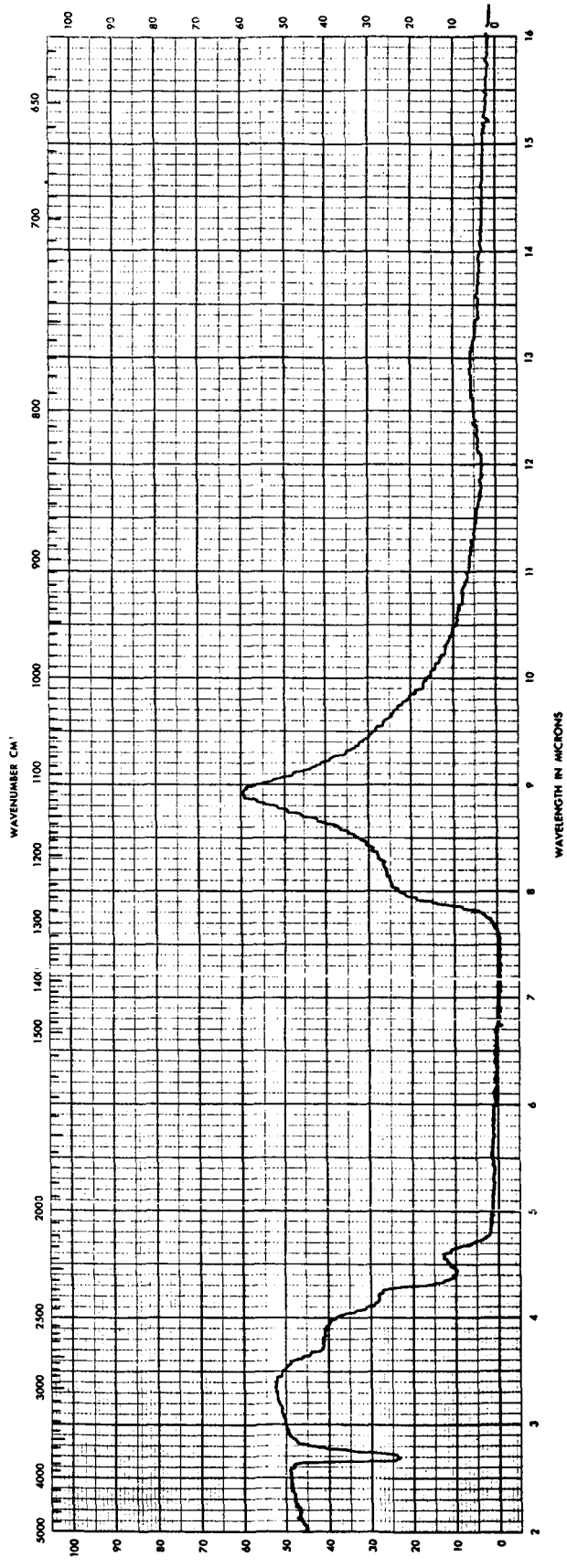

Figure 19. Double-beam Reflection Spectra of Fe_3O_4

is believed to be new in that the infrared reflectance spectra studies have not been found in the literature.

6.2.2 Fe_2O_3-B_2O_3 Ferrite Films

An effort was made to obtain commercial sources of Fe_3O_4 material that would have a higher degree of purity. Surprisingly, these efforts were not as successful as expected. An Fe_2O_3 powder of 99.995%, however, was obtained from Koch-Light Lab., Ltd., England. The material is red and nonmagnetic. Spectrographic analysis of the material showed that no impurities were detected. The minimum detectable limit is 0.001%. A mixture of 95% Fe_2O_3 - 5% B_2O_3 was deposited from a tungsten boat onto the ends of graphite electrodes. The spectrographic analysis showed that the film did have 0.01-0.05% boron, 0.001-0.005% phosphous, and 0.5-4.0% tungsten. The boron impurity was expected to appear, but not the phosphorous. The appearance of the stronger amount of tungsten indicates that Fe_2O_3 may exhibit some degree of reaction with the tungsten boat. The following impurities were searched, but not detected: Al, Sb, As, Ba, Bi, Cr, Co, Cu, Pb, Li, Mg, Mn, Mo, Ni, Si, Ag, Na, Ta, Sn, V, and Zn.

Mixtures of Fe_2O_3 - B_2O_3 ranged respectively from 100%-0%, 99%-1%, 95%-5%, and 90%-10% by weight. The resulting films of the 100%-0% and 99%-1% mixtures were metallic and low resistivity. The 95%-5% and 90%-10% mixtures resulted in films that were dark and responded to a d-c magnetic field. The X-ray spectrographic curves of the films did not show any diffraction lines for the samples regardless of treatment. Films from the various mixtures were deposited on fused silica substrates at temperatures

of 200°C, 400°C, 500°C, and 700°C. The thicknesses ranged from 3000 Å to 3.5μ. In each of the cases, none of the films exhibited any crystalline structure. The implications are that either the films are amorphous or consist of a microcrystalline structure undetected by X-ray diffraction techniques. Each of the films, however, was magnetic. Therefore, one major difference of Fe_3O_4 -B_2O_3 and Fe_2O_3 - B_2O_3mixtures used in the vacuum deposition of the films is that, under identical deposition conditions, the resulting films of the Fe_3O_4 mixtures do exhibit some degree of crystallinity, whereas the Fe_2O_3 mixtures do not exhibit any degree of crystallinity. The crystallinity and lack of it cannot be explained at this time for the two mixtures.

6.2.2.1 Magnetic Properties: The magnetic properties of the films have only been partially investigated. This is due to two factors: (1) the initial emphasis has been to surmount the problem of depositing a ferrite in a vacuum without posttreatment; and (2) the measuring equipment, including the experimental magnetic drive and sense coils and proper assembly of electronic equipment, was not yet completed.

An attempt was made to determine dynamic B-H loops (flux density as a function of sinusoidally varying magnetizing force) for the magnetic films. The electronic test setup is shown in figure 20. The purpose of the RC network is to integrate the signal from the coil so that vertical deflection on the oscilloscope is proportional to flux density, B. It was found that the RC network resulted in too much attenuation of the signal; therefore, it has been temporarily removed until a suitable amplifier is available to amplify

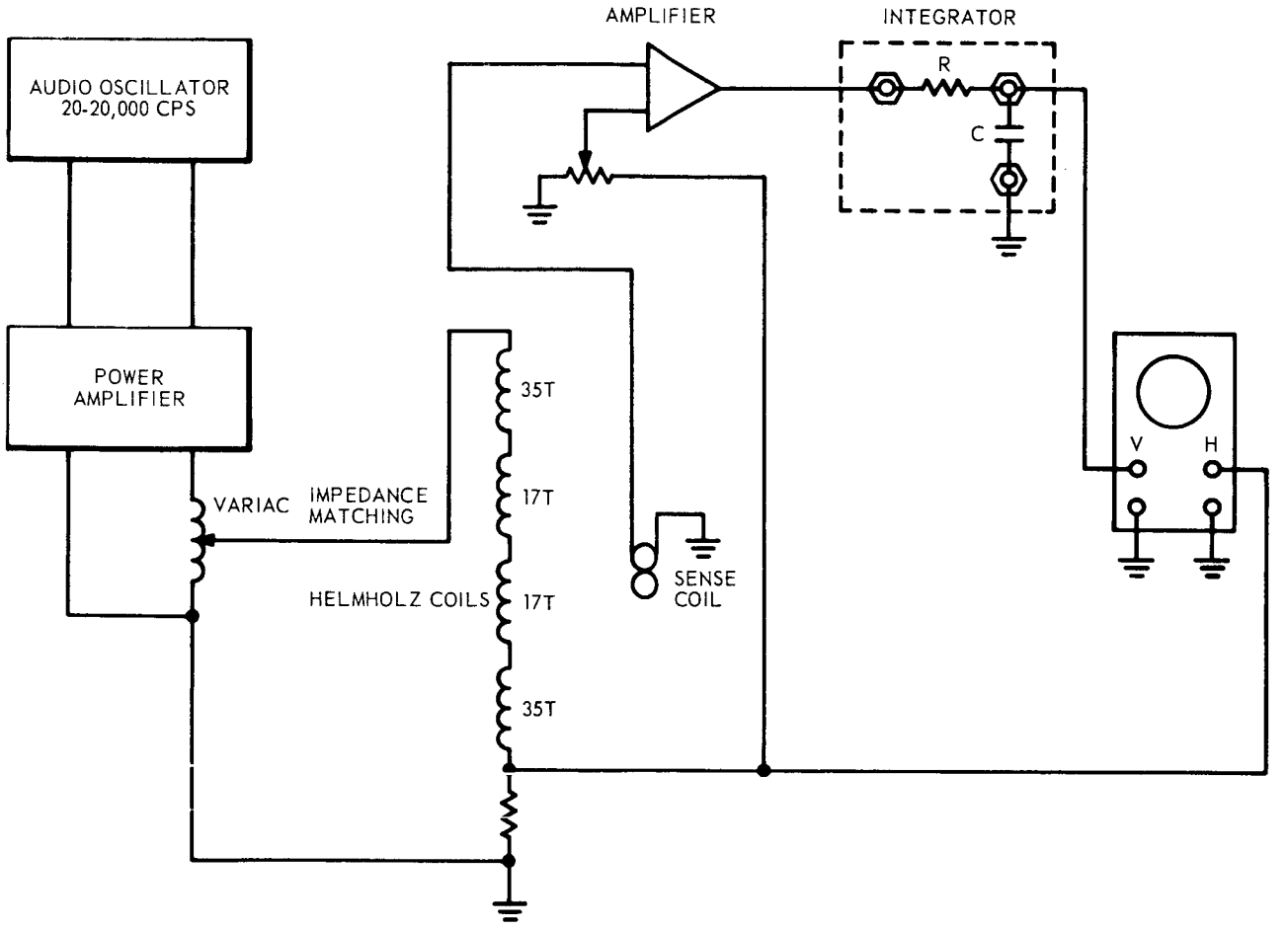

Figure 20. Dynamic B-H Loop Test Setup

the sensing coil signal. Consequently, the vertical scope deflection is proportional to the time rate of change of flux density, dB/dt, for the data taken thus far.

The horizontal scope deflection is proportional to the magnetizing force, H, of the driving coil because the voltage supplied to the horizontal input to the scope is proportional to the current (or ampere-turns) in the driving coil.

Thus, the oscilloscope trace represents dB/dt vs. H. This curve is useful for comparison because the vertical amplitude is proportional to permeability (μ = dB/dH) at a fixed frequency for different core samples.

The core samples, in the form of a square plate, are mounted in contact with the driven or sensing coil (planar figure "8" configuration[7]) shown in figure 21. The driving coil is a modified four-ring Helmholz coil[7] driven by an audio oscillator and amplifier.

It was found that films must be at least 3000 Å thick to produce an appreciable dB/dt response in the above test apparatus for frequencies between 20 and 20,000 cps, although all the films produced were attracted to d-c magnets.

Figure 22 (a and b) shows dB/dt versus H curves for a bulk nickel foil core and an evaporated ferrite film tested in the above apparatus at 600 cps. The magnetic properties of thin nickel films are very similar to bulk characteristics; thus, the nickel foil, which is 12 microns, can be used as a comparative standard. The ferrite film, which is 1.05 microns thick, was formed by evaporating a mixture of 95% Fe_3O_4 and 5% B_2O_3 at a substrate

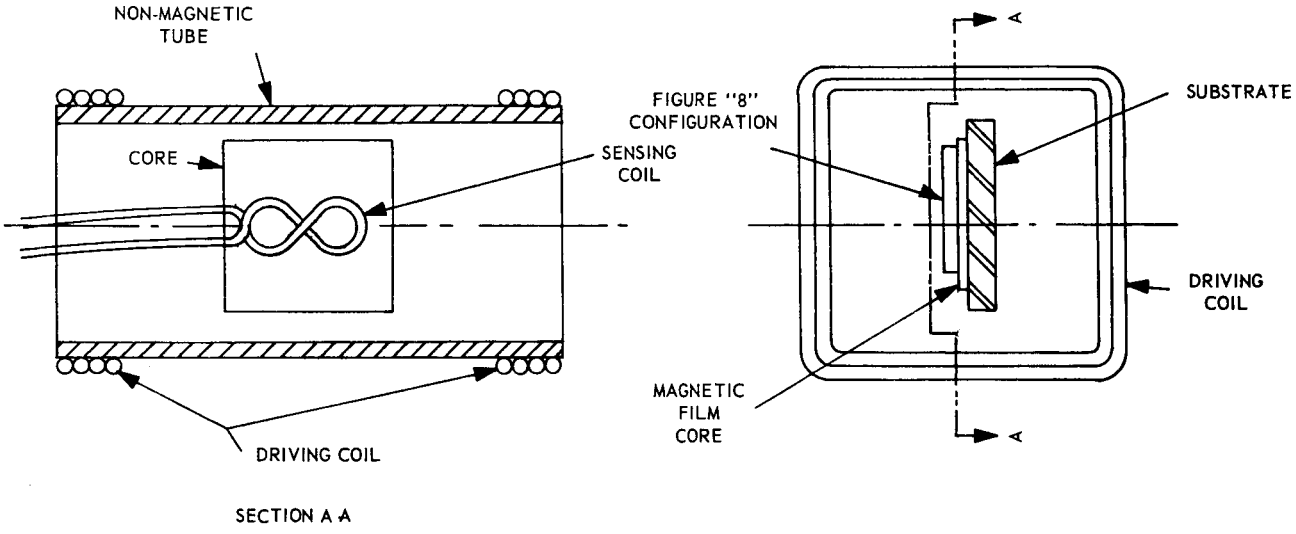

Figure 21. Modified Helmholz Coil

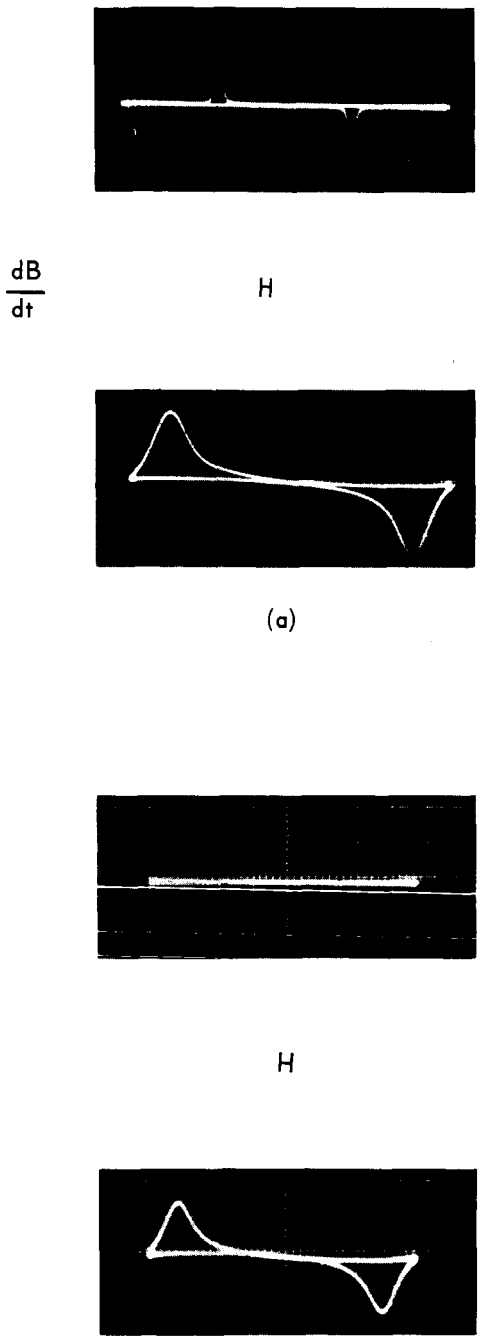

Figure 22. dB/dt Curve at 600 Cycles/Sec of (a) Fe_3O_4 Film Mixtures and (b) Fe_2O_3 Film Mixture (Top) Compared to Nickel Foil (Bottom)

temperature of 200°C. This is shown in figure 22a. The ferrite film in figure 22b is formed from 95% Fe_2O_3 and 5% B_2O_3 deposited on a substrate at 200°C. This film is 1.18 microns thick. In figure 22b, it can be seen that the switching speed of the magnetization of the film is faster because the dB/dt peaks are more sharply resolved. (It must be stated here that the value of the magnetic driving field, the H field, is not known, and must be calibrated for measurement of the magnetic properties of the ferrite films.)

The results obtained so far, as stated earlier, have been limited because of instrumentation. Some significant information, however, has been achieved. The coercive field force causing the switching of the B-H loops appears to be independent of the frequency of the switching field of the driving field. This effect can be seen in figure 23. A series of oscillographs are shown in sequence as a function of frequency. The driving field was kept nearly as constant as possible; the gross effect, however, was sought here. The main effect is that, in the audio frequency, i.e., from 200 to 10,000 cps, the position of the peaks is independent of the frequency. At 100 cps, the peaks are smaller in magnitude and the coercion force appears to be slightly diminished. At 10,000 cps, the film becomes lossy, and at 20,000 cps, the peak is not well resolved. It is believed, however, that this is caused by the less driving current for the Helmholz coil.

The dB/dt peaks as a function of frequency of the nickel foil are shown in figure 24. The ferrite peaks at 600 cps are shown for reference. The metal foil becomes quite lossy at 2000 cps and 10,000 cps. At 20,000 cps, no effect can be observed. The driving current for the magnetic field, however, is not sufficient to obtain the saturation magnetization.

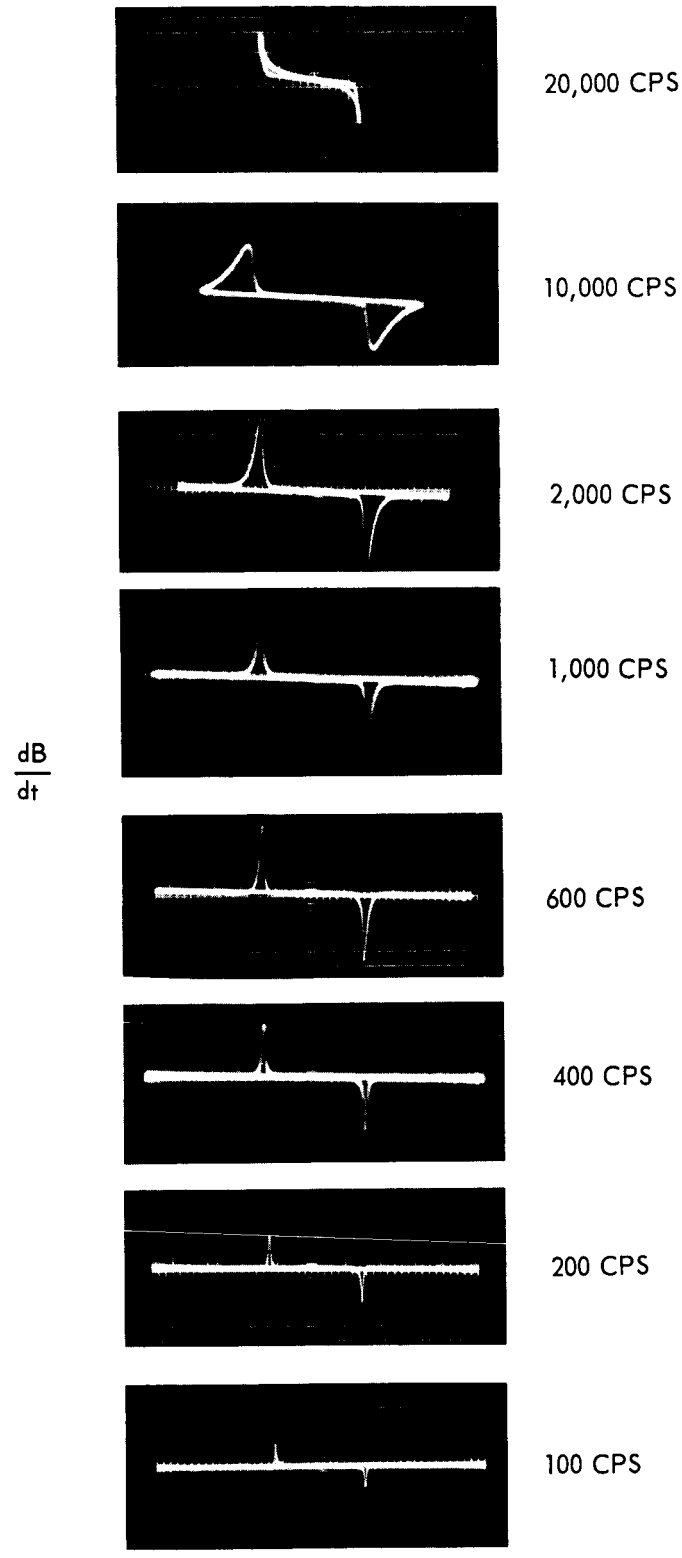

Figure 23. dB/dt Peaks for Ferrite Films at Different Frequencies

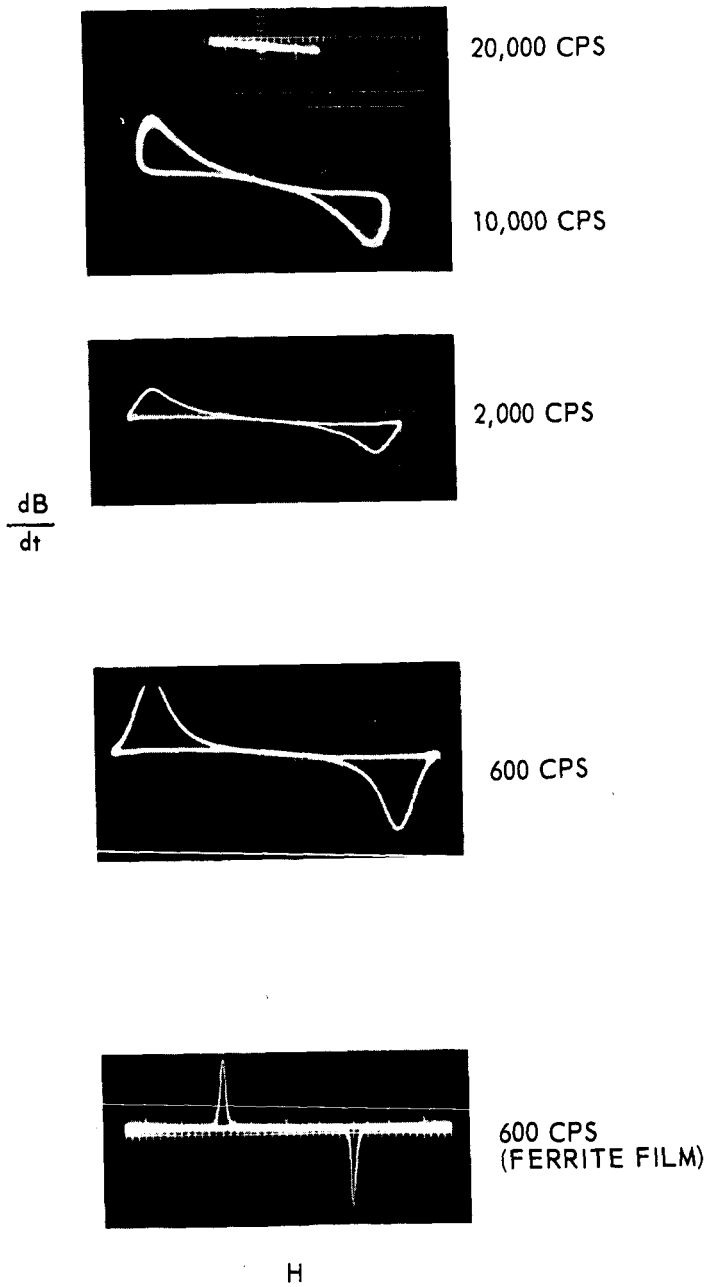

Figure 24. dB/dt Peaks for Nickel Foil at Differant Frequencies

The results reported in this section are preliminary in context. The measured properties, such as the crystallinity, chemical composition, and optical reflectance spectra, as well as the magnetic switching dB/dt peaks, fully corroborate the vacuum-deposited ferrite films.

6.3 Ferrite Core Evaluations

The application of the thin-film ferrites as magnetic core material has been briefly investigated. The description and results of the flat, square, spiral configuration have been reported in this report and in the First Quarterly Report; therefore, further description here has been omitted. To obtain gross effect results, however, a single-turn square coil was used for the following evaluations.

The coil material was a nichrome-copper laminated conductor, and gold wire leads were microbonded to the terminal pads. The substrate material was Corning, code 0211, glass.

The coil resistance was 0.2 ohm, and the following characteristics were measured and are given in table IV. The data was taken from the Boonton, 190-A, Q meter.

For the effect of the ferrite film deposited directly onto the coil having been initially deposited on the substrate, it was found that the resistivity of the ferrite was too low to obtain capacitance and Q measurements for this configuration. Therefore, the ferrite film was coated with an insulating layer of SiO prior to the deposition of the coil. The coil resistance was 0.8 ohms, which accounts for the lower coil Q value. The measured values of the layered ferrite core inductors are shown in table V.

Table IV

ELECTRICAL CHARACTERISTICS OF SINGLE-TURN SQUARE COIL

f mc	C pf	Q	$L = \frac{1}{\omega^2 C}$ μh
69.2	100	25	0.052
100	47	30	0.054
200	10	38	0.064
245 (Resonant frequency)	0	44	--

Table V

ELECTRICAL CHARACTERISTICS OF SINGLE-TURN SQUARE COIL DEPOSITED ON SiO INSULATED FERRITE FILM

f mc	C pf	Q	$L = \frac{1}{\omega^2 C}$ μh
68	100	8.6	0.055
100	45.8	8.0	0.055
200	11.3	6.0	0.056
248.5 (Resonant frequency)	0	5.5	--

The electrical characteristics of the SiO insulated coil-ferrite configuration do not show any inductive effect.

An inductor was fabricated with the single-turn coil deposited first, then the SiO insulating layer, then, finally, the ferrite film.

The electrical parameters were measured and are shown in table VI. The results here indicate that the SiO-ferrite films do not improve the Q of the inductor. Although the capacitances of the two configurations agree at the same frequency, the Q of the SiO-ferrite coated coil does not appear to be frequency dependent as the uncoated coil.

The final configuration of inductor pattern was as follows: The single-turn coil was deposited on one side of the substrate, and then the ferrite was deposited on the opposite surface of the substrate, i.e., a 20-mil insulation glass substrate separated the coil and the ferrite film. The results are shown in table VII. The Q of this configuration with respect to the coil without the ferrite has increased at the lower frequencies, and maintained a nearly constant value independent of the frequencies. This effect was also noted on the coil which was deposited on the SiO insulated ferrite. The reason for this effect is not understood. It is obvious, however, that the magnetic properties of the films are not being utilized, and techniques for increasing the coil-ferrite coupling must be further studied.

Figure 25 shows graphically the results of the various inductor configurations in layered form.

Table VI

ELECTRICAL DATA OF COIL ON SUBSTRATE AND COIL COATED WITH SiO AND FERRITE FILMS

Coil on substrate alone			Coil coated with SiO and ferrite films		
f	C	Q	f	C	Q
mc	pf		mc	pf	
62.7	100	29	62.7	100	24.0
100	36.9	31.8	100	38.5	29.5
200	8.7	39	200	8.82	31.0
223.8 (Resonant frequency)	0	41	227.5	.0	32.0

Table VII

ELECTRICAL PROPERTIES OF SINGLE-TURN COIL, GLASS SUBSTRATE (20-MIL), FERRITE FILM CONFIGURATION

f mc	C pf	Q
69.6	100	32
100	47.5	38
200	11.1	35.5
250.8 (Resonant frequency)	0	29.5

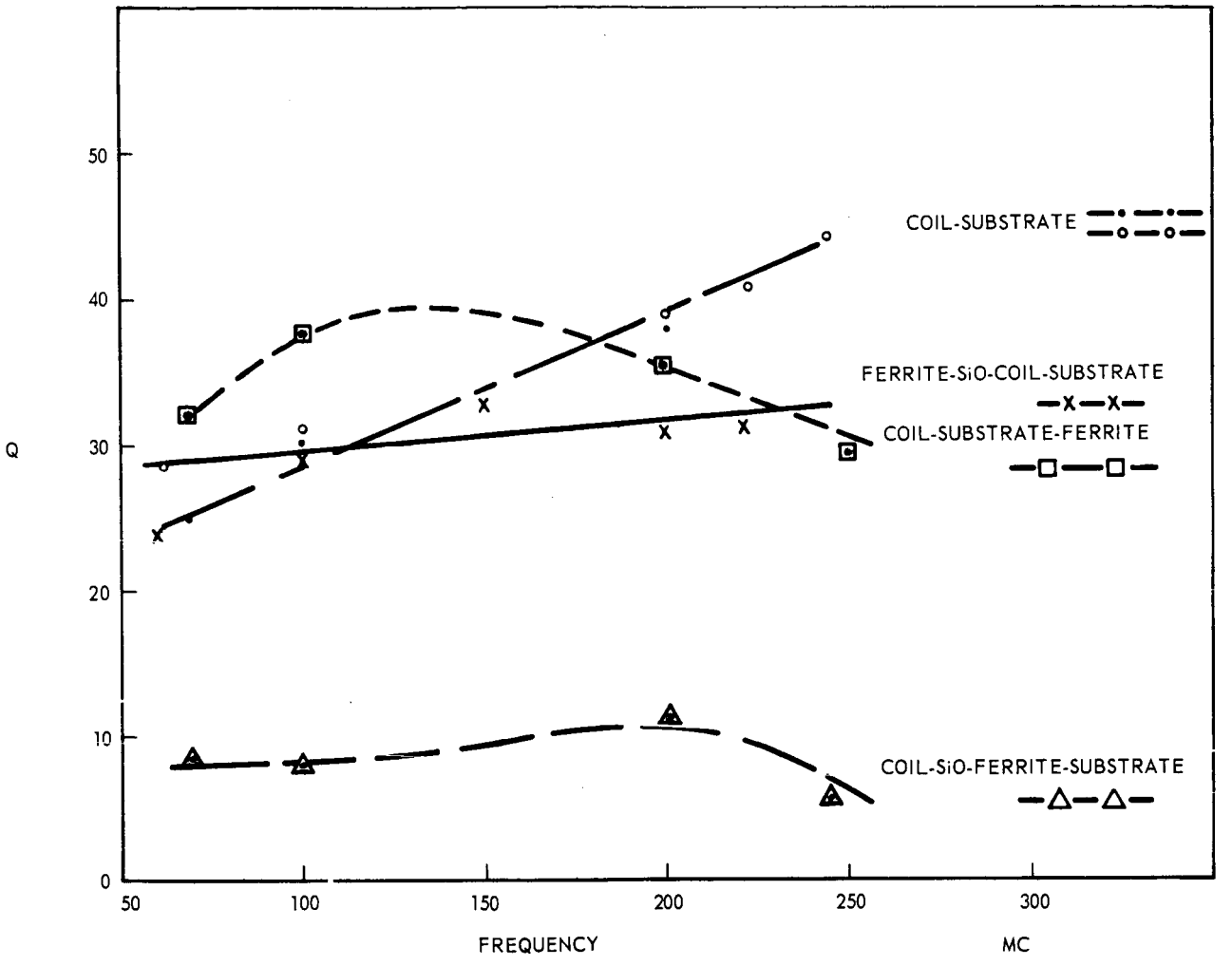

Figure 25. Q as Function of Frequency for Various Coil-ferrite Combinations

6.4 Iron Core Films

The investigations were initiated on the formation of iron film. The inductors discussed in section 5 of this report were deposited on thin metal foil of high permeability. This foil is generally used for shielding. The coils were insulated from the metal with a 20,000-angstrom film of silicon monoxide. The capacitance between the coil turns and the foil swamped out all inductive effects.

This type of foil was also placed under substrates with coils on them. The results are given in table VIII. The data was not noticeably affected by different substrates. The result of the metal foil lowered the inductance value and the Q value, and raised the self-resonant frequencies. This means that more losses are being introduced to the inductor, as well as some of the coil being effectually shunted. This would shorten the coil and verify the obtaining of less inductance with a higher self-resonant frequency.

It is known that bulk iron material will not retain its high-permeability characteristics at these frequencies. Obviously, the foil follows these bulk properties.

Whether the very thin deposited layer of iron will eliminate the eddy current and hysteresis losses has not yet been determined. The possible problem of film sauration at too low a flux density to be useful also remains.

The deposition and evaluation of actual iron films have been generally preempted by the more promising ferrite film work. This effort is now underway, and the answers to the above questions should be answered soon.

Table VIII

ELECTRICAL EFFECTS OF SINGLE-TURN COIL
ON SUBSTRATE ON METAL FOIL

Notes	Coil on substrate alone			Coil on substrate on metal foil		
	f (mc)	L (μh)	Q	f (mc)	L (μh)	Q
A	30	0.624	11.1	30	0.442	5
B	73.4		19	92		5
C	70	0.63	8	30	0.434	5
D	73		13.2	95		5

Notes:

A Englehard quartz substrate (40 mils thick).

B Self-resonant frequency.

C Corning 0211 glass substrate (20 mils thick).

D Self-resonant frequency.

6.5 Program for the Next Quarter

The results presented in this section concerning the investigations of vacuum-deposited thin-film ferrites are preliminary. The electrical and magnetic properties of the films will be measured with the B-H loop-tracer. The coil-ferrite layered configuration will be investigated to obtain a higher degree of magnetic coupling.

The iron films are in the process of being deposited, and results should be determined during this quarter. So far, investigations have not proved promising for these films.

7. CONCLUSIONS

Field effect has been obtained in many different semiconductor films, and those which show the most promise of forming a high-frequency TFT have been selected. The work will now emphasize attempting to optimize the thin-film fabrication techniques for these semiconductors. The metal base transistor and diode efforts are progressing nicely. When the junctions are sufficiently developed, transistor formation will be attempted. The diode work will continue independently and will feed into the varacator study. High-frequency thin-film capacitors will not present a problem in the program; therefore, this effort is considered completed. Inductors seem to form straightforward, promising, passive components in thin-film form. Information on film resistance as a function of frequency, as it effects Q value, will be obtained. Ferrite-core research for high-frequency high-permeability usage has been encouraging. During the next quarter, more effort in defining and measuring the magnetic properties of the thin films of ferrite will be expended.

8. REFERENCES

1. H. L. Wilson and W. A. Gutierrez, Journal of the Electro-Chemical Soc., Vol. 112, No. 1, Jan. 1965.

2. J. M. C. Dukes, Printed Circuits, Their Design and Application MacDonald, London, 1961.

3. H. E. Bryan, "Printed Inductors and Capacitors," Tele-Tech 14, No. 12, Dec. 1955, p. 68.

4. H. H. Skilling, Fundamentals of Electric Waves, Second Edition, John Wiley and Sons. Inc., New York, 1948.

5. H. G. Dill, "Designing Inductors for Thin-film Applications," Electronic Design 12, February 17, 1964.

6. F. Vratny and J. J. Kokalas, "The Reflectance Spectra of Metallic Oxides in the 300 + 01000 Millimicron Region," Applied Spectroscopy, 16, 176 (1962).

7. "Memory Study and Development Program," Final Report on Contract No. AF 30(635)-1401, 1959.

8. C. A. Neugebauer, "The Saturation Magnetization of Nickel Films of Thickness Less Than 100Å," The Structure and Properties of Thin Films. Edited by C. A. Neugebauer and others. John Wiley and Sons, 1965.

Senior personnel who participated in work on this contract this quarter are:

Dr. Charles Feldman

Mr. William A. Gutierrez

Mr. Michael Hacskaylo

Mr. Richard C. Smith

Mr. Wendell Spence

Mr. Herbert L. Wilson

Mr. Barry J. Weiner

Prepared by: Barry J. Weiner

Barry J. Weiner
Liaison Project Engineer

Approved by: M. Hamby for C. Feldman

Charles Feldman, Manager
Physical Electronics Laboratory

E. L. Ditz, Manager
Space Research and Technology Center

Paul E. Ritt, Vice President
Research and Engineering